AD-A186 254 ANALYSIS OF THREE-DIMENSIONAL VISCOUS INTERNAL FLOWS 1/1
(U) CINCINNATI UNIV OH DEPT OF AEROSPACE ENGINEERING
AND ENGINEER K N GHIA ET AL 31 MAR 87
UNCLASSIFIED UC-ASE-87-6-71 AFOSR-TR-87-1215 F/G 20/4 NL

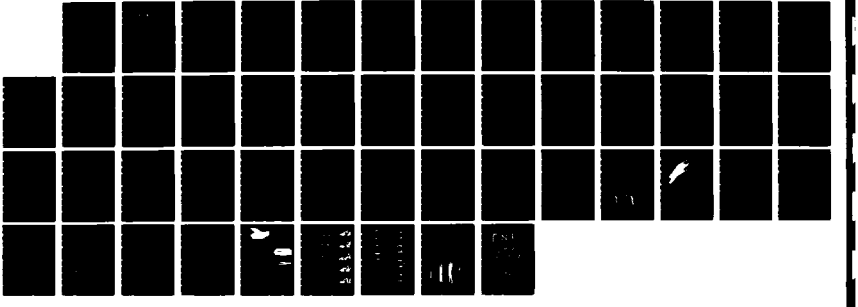

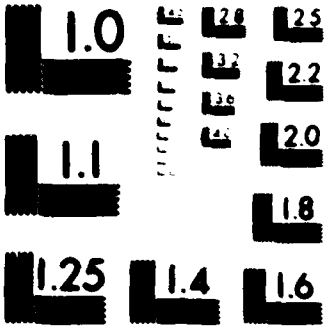

SSIFIED

CLASSIFICATION OF THIS PAGE

DTIC FILE COPY

DOCUMENTATION PAGE

1a. REPORT Uncl	AD-A186 254
1b. RESTRICTIVE MARKINGS	
2a. SECU	
3. DISTRIBUTION/AVAILABILITY OF REPORT: Approved for Public Release; Distribution Unlimited.	
2b. DECLASSIFICATION/DOWNGRADING SCHEDULE	
4. PERFORMING ORGANIZATION REPORT NUMBER(S): 87-6-~~60~~ 71	5. MONITORING ORGANIZATION REPORT NUMBER(S): AFOSR-TR- 87-1215
6a. NAME OF PERFORMING ORGANIZATION: University of Cincinnati	6b. OFFICE SYMBOL (If applicable):
7a. NAME OF MONITORING ORGANIZATION: Air Force Office of Scientific Research/NA	
6c. ADDRESS (City, State and ZIP Code): *Dept. of Aerospace Engg. & Engg. Mechanics **Dept. of Mechanical & Industrial Engineering Univ. of Cincinnati, Cincinnati, OH 45221	7b. ADDRESS (City, State and ZIP Code): Building 410 Bolling Air Force Base, DC 20332
8a. NAME OF FUNDING/SPONSORING ORGANIZATION Air Force Office of Scientific Research	8b. OFFICE SYMBOL (If applicable): NA
9. PROCUREMENT INSTRUMENT IDENTIFICATION NUMBER: AFOSR 85-0231	
8c. ADDRESS (City, State and ZIP Code): Building 410 Bolling Air Force Base, DC 20332	10. SOURCE OF FUNDING NOS.

PROGRAM ELEMENT NO.	PROJECT NO.	TASK NO.	WORK UNIT NO.
61102	2307	A4 ~~2307/A4~~	

11. TITLE (Include Security Classification): Analysis of Three-Dimensional Viscous Internal Flows (Unclassified)

12. PERSONAL AUTHOR(S): Kirti N. Ghia* and Urmila Ghia**

13a. TYPE OF REPORT	13b. TIME COVERED	14. DATE OF REPORT (Yr., Mo., Day)	15. PAGE COUNT
Final Report	FROM July 1985 TO Sept. 1986	1987, March, 31	45

16. SUPPLEMENTARY NOTATION

17 COSATI CODES			18. SUBJECT TERMS (Continue on reverse if necessary and identify by block number)
FIELD	GROUP	SUB. GR.	
			Viscous Flows, Interacting PNS Equations, Flow Separation, Multi-Block Structured Grids, Unsteady Flows, Three-Dimensional Flows

19. ABSTRACT (Continue on reverse if necessary and identify by block number)

A fifteen-month multi-tasked research project was pursued by the present investigators to study complex viscous flows under AFOSR sponsorship between July 1985 and September 1986. The major objective of this study was to acquire improved understanding of viscous flows and to develop basic computational methods for efficient determination of 2-D/3-D subsonic and incompressible flows. Two major analyses were pursued. These include the Interacting Parabolized Navier-Stokes (IPNS) analysis for steady flows and the full Navier-Stokes (NS) analysis for direct simulation of unsteady flows. The IPNS analysis developed employs no ad hoc artificial dissipation and, in spite of being a density-based formulation, performs well even for very low Mach numbers. The applications considered include 2-D cascades and channels of simple geometry. The flow solutions are well behaved in the presence of sharp leading edges and trailing edges, as well as in the presence of reversed

20. DISTRIBUTION/AVAILABILITY OF ABSTRACT	21. ABSTRACT SECURITY CLASSIFICATION
UNCLASSIFIED/UNLIMITED ☒ SAME AS RPT ☐ DTIC USERS ☐	Unclassified

22a. NAME OF RESPONSIBLE INDIVIDUAL	22b. TELEPHONE NUMBER (Include Area Code)	22c. OFFICE SYMBOL
Dr. James D. Wilson	202-767-4935	NA

DD FORM 1473, 83 APR EDITION OF 1 JAN 73 IS OBSOLETE.

UNCLASSIFIED
SECURITY CLASSIFICATION OF THIS PAGE

19. ABSTRACT (Continued)

flow. The complete unsteady NS analysis is based on direct-solution methodology and has proved to be very robust and efficient. It has been applied to analyze high-incidence aerodynamics of symmetric as well as cambered Joukowski airfoils, and has yielded very interesting results regarding multiple incommensurate frequencies in the large-time behavior of the flow and, hence, regarding the theory of strange attractors and chaos. The corresponding 3-D analysis appears well on its way and looks very promising. All of this research relies heavily on usage of the supercomputers at the NASA Research Centers, in addition to all the various computing and graphics facilities at the University of Cincinnati. Both the 2-D analyses developed are reasonably mature now and should be useful for examining realistic flow phenomena.

18. SUBJECT TERMS (Continued)

Semi-Implicit and Implicit Numerical Methods
Block-Gaussian Elimination Method
Neumann Pressure Problem
Supercomputer Application

REPORT NO. AFL 87-6-70

AFOSR-TR- 87-1215

ANALYSIS OF THREE-DIMENSIONAL VISOCUS INTERNAL FLOWS

K.N. GHIA
AND
U. GHIA

This research was supported by the Air Force Office of Scientific Research, under AFOSR Grant No. 85-0231.

June 1987

ANALYSIS OF THREE-DIMENSIONAL VISCOUS INTERNAL FLOWS

K.N. GHIA*
Department of Aerospace Engineering and Engineering Mechanics

and

U. GHIA*
Department of Mechanical and Industrial Engineering

University of Cincinnati
Cincinnati, Ohio

This research was supported by the Air Force Office of Scientific Research, Bolling Air Force Base, under AFOSR Grant No. 85-0231, with Dr. James D. Wilson as Technical Monitor.

* Professor.

ABSTRACT

A fifteen-month multi-tasked research project was pursued by the present investigators to study complex viscous flows under AFOSR sponsorship between July 1985 and September 1986. The major objective of this study was to acquire improved understanding of viscous flows and to develop basic computational methods for efficient determination of 2-D/3-D subsonic and incompressible flows. Two major analyses were pursued. These include the Interacting Parabolized Navier-Stokes (IPNS) analysis for steady flows and the full Navier-Stokes (NS) analysis for direct simulation of unsteady flows. The IPNS analysis developed employs no ad hoc artificial dissipation and, in spite of being a density-based formulation, performs well even for very low Mach numbers. The applications considered include 2-D cascades and channels of simple geometry. The flow solutions are well behaved in the presence of sharp leading edges and trailing edges, as well as in the presence of reversed flow. The complete unsteady NS analysis is based on direct-solution methodology and has proved to be very robust and efficient. It has been applied to analyze high-incidence aerodynamics of symmetric as well as cambered Joukowski airfoils, and has yielded very interesting results regarding multiple incommensurate frequencies in the large-time behavior of the flow and, hence, regarding the theory of strange attractors and chaos. The corresponding 3-D analysis appears well on its way and looks very promising. All of this research relies heavily on usage of the supercomputers at the NASA Research Centers, in addition to all the various computing and graphics facilities at the University of Cincinnati. Both the 2-D analyses developed are reasonably mature now and should be useful for examining realistic flow phenomena.

TABLE OF CONTENTS

LIST OF FIGURES

SECTION 1

OBJECTIVES

The development of computational fluid dynamics (CFD) analyses for complex viscous interacting flows was pursued by the present investigators during July 1985 - September 1986. The major thrust of the work was in the development of two analyses, which are briefly outlined as under:

Viscous Interacting Analysis: Internal Flows

Subsonic flows are essentially elliptic in character. However, in a large class of internal flow applications, streamwise diffusion is negligible, although upstream influences through pressure interactions are significant. These situations can be analyzed and computed more efficiently using the Interacting Parabolized Navier-Stokes (IPNS) model rather than the full Navier-Stokes equations, particularly for steady flow. The IPNS model and the corresponding numerical method were studied, with the objective of developing an efficient procedure of desirable versatility for use in studying flows in diffusers, cascades, etc.

Unsteady Navier-Stokes Analysis: Internal and External Flows

Unsteady separation and vorticity interactions in self-excited and forced unsteady flows are important fundamental phenomena which occur in internal as well as external flows. Unsteady separation in large-vortex dominated flows is particularly important in external flows. The underlying physical mechanisms were examined by analyzing flows exhibiting these phenomena, with the help of the complete unsteady Navier-Stokes equations solved using a direct (fully implicit) numerical technique.

Additional items such as grid generation and development of solution algorithms were also studied to further aid the above two analyses. These items contribute significantly to basic research even by themselves. Moreover, these essential elements were needed for successfully developing the two main analyses.

SECTION 2

DESCRIPTION OF SIGNIFICANT ACCOMPLISHMENTS

All of the areas of research proposed for study were pursued during this 15-month grant period. The progress achieved in each of these areas is briefly described in this section.

2.1 Composite Generation of Multi-Block Grids for Subsonic Cascades

Examination of the basic grids for cascades shows that a C-grid can adequately resolve the boundary layers on the blades as well as the wakes downstream and is satisfactory everywhere except in the region upstream of the blades. In this region, the grid density decreases rapidly with distance upstream of the front stagnation point. On the other hand, an H-grid is generally satisfactory in this region and also facilitates implementation of the repeating boundary condition for cascade flows. For cascades with minimal stagger and blades with thin leading edges, the H-grid is not highly skewed. But when the blades possess thick rounded leading edges typical of turbine cascades, the H-grid becomes highly skewed in the leading-edge regions (Fig. 1). Earlier, K. Ghia and U. Ghia [1982] had suggested an approach for improving a basic C-grid for use with cascades. This consisted of deleting a segment of the C-grid in the upstream region and patching a segment of an H-grid onto the remainder of the C-grid, as shown in Fig. 2. The resulting coordinates appear satisfactory everywhere. It should be noted that this hybrid coordinate system contains two five-sided cells which require special consideration.

The concept of C-H hybrid grids for cascades was pursued further by U. Ghia et al. [1983]. The main result of that effort is shown in Fig. 3. Here, a C-grid encompasses a narrow region in the vicinity of the lower

blade and approximately includes the wake region. Similarly, a C-grid also covers the corresponding repeating region around the upper blade. The remainder of the flow domain between the blades is then occupied by a sequence of three H-grid blocks. This led to a five-block grid system for the cascade. The grid in each of the five blocks was generated separately using numerical solution of elliptic partial differential equations governing the coordinate transformation. Continuity across the block interfaces was maintained by a single visit to each block, performed in a specific sequence. First, the C-grid portions of the cascade coordinates were generated, using appropriate forcing functions to provide resolution of the blade boundary layers. The resultant clustering near the outer boundary of the C-grid blocks was employed to determine the forcing functions for the grids in the adjoining H-grid blocks, leading to an overall grid system that is continuous everywhere. This procedure also circumvented the difficulties to be expected with the two five-sided cells appearing in this hybrid grid. However, the procedure required knowledge of the grid-point distribution at all block interfaces; this constituted a major difficulty, especially so far as the solution for the flow itself was concerned.

Work performed under the present grant has resulted in the development of a composite solution procedure which does not employ, or require, any information along block interfaces. The boundaries of the computational region correspond only to actual boundaries in the physical plane. All information along physical-block interfaces is obtained as part of the evolving overall solution. Therefore, no special iterative measures are required at these interfaces. The first step towards developing this procedure was the appropriate representation of the physical region in the computational domain. The earlier 3-D computational-domain representation

(Fig. 3) by U. Ghia et al. [1983] of the 2-D hybrid grid was very useful but was computationally inefficient. The present representation of the 2-D physical problem retains a 2-D computational region. Only the true boundaries of the physical region appear as boundaries in the computational plane; no block interfaces are exposed as computational boundaries. The resultant multi-rectangular computational-region representation also paves the way for appropriate treatment of the five-sided cells appearing in the hybrid grid. Finally, this representation is very well suited for the numerical solution of the coordinate-generation equations, as well as the flow equations, even by implicit methods such as ADI. The various blocks used in the hybrid grid for a staggered cascade are shown in Fig. 4 which shows mainly the boundaries of these blocks. The corresponding computational region is shown in Fig. 5. With this arrangement, the grid is developed simultaneously in all the blocks without any special consideration of block interfaces. This is a unique feature of the present multi-block domain-decomposition procedure. An invited paper based on some preliminary results from this work was presented by U. Ghia et al. [1985]; a written version of the paper was also prepared later by U. Ghia et al. [1986].

2.2 Steady Flows with Strong Upstream Interactions

In this effort, a reduced form of the governing equations has been developed which can capture much of the physics, while requiring less computer resources than the full Navier-Stokes equations. It belongs to the category of semi-elliptic analyses, one form of which was proposed and employed earlier by U. Ghia et al. [1981]. The formulation holds greatest promise for high-Re steady flows with a predominant flow direction. It should be mentioned, however, that the procedure can be extended easily to

include consideration of unsteady flows. But the most unique feature of the method is its ability to compute low-Mach number flows. Although it is a density-based method, it is not plagued by computational difficulties for $M_\infty \to 0$, as are the other density-based methods available. Also, no use is made of any externally added artificial viscosity. The method is applicable to 3-D flows as well.

The governing differential equations used are derived from the Navier-Stokes equations, together with the continuity equation and the energy equation, for steady flow of a compressible fluid. With Cartesian decomposition of the vector quantities, these equations are expressed, in terms of a general coordinate system (ξ,η), in the strong-conservation law (SCL) form. Expressing the transformed governing differential equations in the SCL form requires that the coordinate transformation metrics satisfy a set of geometric conservation relations. In an analytical formulation, these are identically satisfied. In a discretized formulation, satisfaction of these relations is ensured by the use of appropriate differencing for the metrics.

The semi-elliptic formulation developed in the present work is obtained by invoking the approximation that, for flows with a predominant flow direction, streamwise diffusion is negligible relative to normal diffusion. Nevertheless, a large class of flows, for which streamwise diffusion may well be negligible, are significantly influenced by upstream interactions, and may not be adequately represented by mathematically parabolic equations. In the present formulation, upstream interaction is provided for via appropriate treatment of the streamwise pressure gradient term. Hence, the formulation is also termed an <u>interacting parabolized Navier-Stokes (IPNS) model</u>. The viscous-inviscid interaction is included by composite

consideration of the viscous and inviscid flow regions through the use of the PNS equations; upstream interactions are propagated and included through the pressure field.

For the subsonic flows considered, the total pressure, total temperature and streamline slope are prescribed at inflow and the static pressure is prescribed at outflow. At the wall-wall boundaries, the conditions of zero slip and zero suction/injection, together with a specified temperature condition, provide a total of six boundary conditions. The one additional boundary condition needed is provided by an approximate form of the normal momentum equation obtained by neglecting the viscous terms in that equation. This last condition is applied in the cells adjacent to the wall, rather than at the wall itself, thus avoiding the need for any one-sided differences for the normal derivatives. The wake-wake boundaries are the periodic boundaries occurring in cascade flows. The periodicity condition requires that the corresponding values of all four flow variables, and the η-derivatives, u_η, v_η and T_η, of the velocities and temperature which are governed by second-order differential equations, be the same at corresponding periodic points along the wake boundaries. It is important to mention that, in terms of the conserved variables (ρ, ρu, ρv, ρe_t) comprising the solution vector $\bar{Q}$, the repeating condition on the η-derivatives must be satisfied for all four elements of $\bar{Q}_\eta$.

The analysis was employed to determine the flow in several channel and cascade configurations. Some of the results obtained are presented here in terms of the two most sensitive quantities, namely, the static pressure and wall shear. Unless otherwise stated, the Mach number M_∞ is approximately 0.008.

Figure 6 shows the distribution of the surface pressure p_b ($= p_{w_{inlet}} - p_w$) and wall-shear parameter, τ_w ($= \partial u_s/\partial n$), obtained for a constricted channel with $t_{max}/h = 0.2$ and $Re = 1500$. Of particular significance is the presence of a finite region of small reversed flow indicated by negative τ_w downstream of the constriction and the completely non-singular behavior of the present IPNS solution for this configuration with upstream interaction.

The performance of the IPNS model in the presence of sharp leading and trailing edges was evaluated by application of the model to a cascade of finite flat plates. Figure 7 shows the distribution of the pressure p_b and shear parameter τ_w for Re ranging from 1500 to 15,000. Through all the highly nonlinear behavior of the flow variables, including that due to abrupt change in the boundary conditions across the leading edge (LE) and the trailing edge (TE), the solution of the IPNS model is quite regular as upstream interactions are appropriately included in it.

The distributions of p_b and τ_w are shown in Fig. 8 for parabolic-arc airfoils for various thickness ratios (Fig. 8a) and for various Reynolds numbers (Fig. 8b). The effect of varying M_∞ up to nearly 0.5 has also been examined. It is found to be minimal on the shear parameter τ_w, but becomes evident in the pressure distribution at the highest value of M_∞ considered. Figure 8c shows the static pressure contours for the case with $M_\infty = 0.49$, $Re = 15,000$. The high-pressure region localized near the LE is evident from the concentration of the contours in this region, as is the more widespread low-pressure regions downstream of the position of maximum thickness. From

the values of the pressure along these contours, it is clear that the pressure varies rather minimally over the airfoil surface. Nevertheless, these variations have been very accurately computed in order to produce the contours which are well behaved and conform to the physics of this flow, especially in the LE and TE regions.

Application to these various flow configurations served to demonstrate that the technique is viable for flows with strong interactions occurring due to boundary-layer separation or the presence of sharp leading/trailing edges. It is important to recall that the procedure developed uses no externally added artificial viscosity and is capable of producing satisfactory solutions for compressible (subsonic) viscous flows, with no modification needed for analyzing nearly incompressible flow as well.

A paper based on these results was presented by U. Ghia et al. [1985]; a written version of the paper was also prepared later by U. Ghia et al. [1986].

2.3 Unsteady 2-D Navier-Stokes Analysis

The simulation of 2-D flows with self-sustained unsteadiness has been continued using the direct solution of the unsteady 2-D Navier-Stokes equations. In addition to determining the basic flow solution, the time-dependent aerodynamic lift, drag and moment coefficients were also obtained for flow past airfoils at high incidence. Effort was also made to understand the observed quasiperiodicity and bring forth any possible similarity with strange attractors.

Symmetric Joukowski Airfoil

A 12 percent thick symmetric Joukowski airfoil is used in this study as it has two especially attractive features. (i) The Joukowski airfoil can be accurately represented using conformal transformations; the details of these and the clustering transformations used, as well as the total analysis, were given by K. Ghia et al. [1985a]. (ii) The presence of a sharp TE leads to a much stronger interacting region and, hence, truly tests the analysis developed. This unsteady Navier-Stokes analysis and the corresponding numerical method are used to study three flow configurations in detail. All of these configurations have the same Re = 1,000 but the value of the free-stream incidence angle α_f varies such that α_f = 15°, 30° and 53°, respectively. For the high angle-of-attack case with α_f = 53°, the Joukowski airfoil appears, to the oncoming stream, as an apparent bluff body. The massively separated vortex-dominated flow in the post-stall regime for this configuration of the Joukowski airfoil is exceedingly complex and, from the results available so far, it is feasible to conjecture two hypotheses; see Fig. 11. One possibility is that the solution has still not asymptoted to an exact limit cycle but may do so subsequently. The second possibility, based on the results for α_f = 30°, is that the solution may asymptote to a quasiperiodic state, with anywhere from 3 to 8 incommensurate frequencies. The second hypothesis is more likely to prevail.

Limit Cycle Analysis

Originally, the aerodynamic coefficients were computed only at intervals of 0.1 characteristic time. This was quite satisfactory for qualitative assessment of the flow evolution but too coarse for its detailed analysis. Subsequently, the computer program has been modified to provide

the coefficients of lift C_L, drag C_D and moment C_M (nose-up positive about the quarter-chord point) at every Δt increment. The configuration with $\alpha_f = 15°$, which requires minimum time to reach the time-asymptotic limit cycle solution, has been completely recomputed, using a slightly improved grid near the TE. The flow configuration with $\alpha_f = 30°$ has been recomputed between t = 45 and t = 58, whereas, due to limitation of availability of CPU time on the host computer system, the configuration with $\alpha_f = 53°$ is currently available with C_L, C_D and C_M computations at time intervals of 0.1 only. Figures 9a,b,c show C_L, C_D and C_M corresponding to α_f=15°. As seen in this figure, C_L rises initially but drops very sharply during the transient phase and asymptotes to a near-limit-cycle solution corresponding to the dominant frequency for the shedding of vortices from the TE. The L_2-norms of the entire vorticity and stream-function fields were carefully examined to ensure that the near-limit-cycle has been achieved. This limit-cycle solution is an "ordinary attractor", the attractor being the 1-D object to which the phase-space trajectories are attracted at all times. The complete motion is known once the geometry of the attractor is determined. Hence, it is also possible to compute the mean flow by averaging the flow over one complete cycle; similarly, it is possible to determine the Reynolds stresses from first principles, although these computations have not been performed in the present study.

For the flow configuration with α_f=30°, the physics changes dramatically, as seen in Figs. 10a,b,c. The curves for the force coefficients show that one limit cycle consists of two TE vortices sheddings. There are now two shedding frequencies, or modes, associated

with this more complex attractor. As shown in Fig. 10a, the first frequency is associated with the shedding which takes place at point 1, whereas the second frequency is associated with the shedding which takes place at point 3. The LE shear layer associated with the first frequency is thinner and more intense, as compared to that associated with the second frequency. The energy now oscillates between the two unstable modes through a nonlinear coupling. The appearance of subharmonics signifies small modulations in the shedding frequency. This flow field, with its two natural incommensurate frequencies, is referred to as a quasiperiodic flow, also known as "Hopf bifurcation" into an invariant torus. From Fig. 10a, it is clear that the initial state at point 10 of a new cycle is slightly different from that at point 8. If the phase-space trajectories were drawn, this solution may very well show a tendency to fill a rather significant surface area of the torus. Finally, it should be noted that the C_D peaks in Fig. 10b correspond to points 2 and 9 in Fig. 10a.

For the case with α_f=53°, the results obtained up to t=74 may be far from approaching an asymptotic state. Figure 11a shows some resemblance of quasiperiodic flow with three incommensurate frequencies, this fact being further supported by the curves in Figs. 11b, c. From their numerical experiments, Grebogi, Ott and Yorke [1983] have also shown the existence of quasiperiodicity with three incommensurate frequencies. The state of the system at a given time instant in one cycle is not quite repeated at the corresponding time instant in the subsequent cycle. The phase-space portrait, not shown here, is very complex, where the surface has folded repeatedly onto itself, so that it appears to be a strange attractor. This is an indication, although preliminary, that the flow may be exhibiting a route to chaos. Some of the rigorous approaches for characterizing a

strange attractor consist of the determination of (i) the Lyapunov exponent; (ii) the fractal dimension of the attractor, which is related to the number of degrees of freedom; and finally, (iii) the Kolmogorov entropy. These indices still need to be studied thoroughly in order to rigorously analyze the route to chaos in a meaningful way.

The overall state of the total flow system was examined in terms of the frequencies associated with the various sheddings and an invited paper based on these results was presented by K. Ghia et al. [1985b]. A written version of the paper was also prepared by K. Ghia et al. [1986].

Cambered Joukowski Airfoil

The 2-D unsteady flow analysis was continued for a cambered Joukowski airfoil. A typical clustered conformal C-grid, with (230, 46) points, is shown in Fig. 12 for the Göttingen 580 airfoil (i.e., an 11.8 percent thick cambered Joukowski airfoil with a zero-lift angle of attack $\alpha_0 = -5.711°$), at effective flow angle of attack $\alpha_e = 30°$.

Results are obtained for three flow configurations with Re = 1000 and $\alpha_e = 5.711°$, 15° and 30°, the last two being in the stall and post-stall flow regimes, respectively. Here, the effective angle of attack is $\alpha_e = \alpha_f - \alpha_0$, with α_f being the geometric angle of attack between the chord and the free-stream direction.

Figure 13 shows the inviscid starting solution, the grid distribution in the near field and the steady-state stream-function and vorticity contours for the case with Re = 1000 and $\alpha_e = 5.711°$. The stream-function contours show a mildly separated region in the vicinity of the trailing edge (TE). Laminar boundary layers prevail on both the suction and pressure

surfaces, as observed in the vorticity contours, which also show a tongue-like behavior. The streamwise extent of the separated flow near the TE is 0.15c, as compared to approximately 0.4c for the symmetric Joukowski airfoil with $\alpha_e = 5°$, as given by K. Ghia, Osswald and U. Ghia [1985b].

The time history of the lift and drag coefficients C_L and C_D, respectively, is depicted in Fig. 14 for the case with Re = 1000, $\alpha_e = 15°$. A time asymptotic limit-cycle solution evolves by approximately t = 12, as compared to t = 31 for the case of the corresponding symmetric airfoil. K. Ghia et al. [1985b] had defined the period as the time interval required for the L_2-norm of the deviation of the instantaneous state of the flow from a reference initial state to become smaller than a specified tolerance. For the present configuration, the period is established by examining the successive maxima of C_L in Fig. 14. The period associated with this limit-cycle (ordinary attractor) is 1.046 characteristic time units and the corresponding Strouhal number $S_{\alpha_f} = fc\ (\sin \alpha_f)/U_\infty = 0.154$; based on α_e, its value is $S_{\alpha_e} = 0.247$. The corresponding period for the symmetric airfoil is 1.416 and $S_{\alpha_e} = 0.18$. Hence, the effect of camber is to increase the frequency of the periodic shedding of large-scale vortices from the TE region and from the separation zone on the suction surface.

The coefficients of lift C_L and drag C_D for the case with Re = 1000, $\alpha_e = 30°$ are shown in Fig. 15. These curves show that, even at t = 52, the flow has not yet reached an asymptotic state. Also, these curves show that one cycle consists of two TE sheddings. Thus, there are two shedding frequencies associated with this attactor; these correspond to the sheddings

associated with points 1 and 2 in Fig. 15. The LE shear layer associated with the first frequency is thinner and more intense as compared to that associated with the second frequency. This flow field, with its two natural incommensurate frequencies, is again referred to as a quasiperiodic flow. The phase-space portrait is complex and is tending towards being a "strange attractor". The corresponding Poincare section indicates that the attractor may be a thin torus. These results are similar to those of the symmetric airfoil (Fig. 11), except that the C_L history appears more chaotic and does not seem to be tending towards a limit cycle. Also, there is a peak due to the shedding from the LE at point 3; this was not present in the results for the symmetric airfoil. The time instants at which the detailed flow results are presented correspond to the TE-LE-TE sheddings.

The instantaneous stream-function contours, presented in Figs. 16a,c,e,g,i, show massively separated flow, with large eddies present over the suction surface as well as in the wake. Figures 16a,g,i show the presence of multiple separations, whereas Fig. 16c shows the presence of two counterclockwise co-rotating bubbles, aft of the shoulder, towards the TE and these bubbles are in the process of coalescing. The corresponding vorticity contours are shown in Fig. 16b,d,f,h,j and various vortex interactions can be observed from this figure. In Fig. 16b, the TE vortex has just been shed, a new TE vortex intensifies as shown in Fig. 16d and is being just separated from the TE by the growing LE vortex. Figure 16f corresponds to shedding of the LE vortex. The state shown in Fig. 16j corresponds to TE shedding and has features similar to those in Fig. 16b.

The results of this effort may be summarized as follows. Up to the stall regime, camber causes the flow fields to be dominated by the TE geometry. Also, the extent of the separated flow is diminished both in the

streamwise and the lateral dimensions and the shedding frequency is increased. For flow fields in the post-stall regime, the C_L time history becomes more chaotic and shows a peak associated with LE shedding. The computation of the flow field needs to be continued to larger t, to predict its further behaviour with definite assurance. A paper based on these results was presented by Osswald et al. [1986] and appears in the Conference Proceedings.

Circular Cylinder

For flow past airfoils at high angle of attack, the airfoil behaves like a bluff body. The large-scale structure of the separated flow past a bluff body, e.g., a circular cylinder, is not understood well, except at extremely low values of the Reynolds number Re around 120 where Re is based on the cylinder diameter. The understanding of separated flow past the model problem of a circular cylinder is crucial, as it may lead to a better understanding of more complex flows such as separated flow past airfoils with or without solution bifurcations associated with lift hysteresis, symmetry breaking, etc. Also, a thorough knowledge of steady separated flow could aid in analyzing unsteady separated flow leading to incipient transition and, eventually, to chaos.

Hence, the flow past a circular cylinder was computed, first without assuming symmetry. The instantaneous streamlines and vorticity contours are presented in Fig. 17 for Re = 200. The occurrence of the bulge phenomenon for Re = 200 and $t \geq 1.0$, first reported by Bouard and Coutanceau [1980], is also computed satisfactorily. It leads to an alteration in the vorticity contours close to the surface of the cylinder in the separated zone. For the corresponding symmetric configuration with Re = 500, the instantaneous

stream-function and vorticity contours are delineated in Fig. 18 at t = 100, 225, 800 and 1600. The eddy length L, as seen from the stream-function contours, increases from approximately 6 diameters at t = 100 to 27 diameters at t=1600; the asymptotic results of Fornberg [1985] show this length to be 36 diameters. Further, the region between the cylinder and the main eddy grows from about 1 diameter initially to 5 1/2 diameters by t = 1600; the corresponding asymptotic results of Fornberg [1985] show this distance to be approximately 8 diameters. This region can be considered as consisting of two parts: the front part where the separating streamline grows in width as $O(Re^{1/2})$, followed by a 'transition' region in which the growth rate adjusts such that the width can grow as O(Re) in the main eddy. Also, in this transition region, the vorticity increases from zero to the level of nearly uniform vorticity present in the main eddy. The kink in the contours of the vorticity is conjectured to be related to this change in the growth rate of the width of the eddy. The results for the velocity do not show O(1) thickness for both the shear layer past the center of the main eddy and the return jet, as proposed by Smith [1985]; the present results need to be scrutinized further to provide the accurate flow structure. The Navier-Stokes calculations show that, near Re = 500, the translating cylinder drags with it a massive eddy.

These results for flow past cylinder were presented by K. Ghia et al. [1986] at the I.U.T.A.M. Conference; a written version of the paper is to appear in the Conference volume.

2.4 Unsteady Three-Dimensional Navier-Stokes Analysis

The effort directed to this area of study was focused primarily on the careful selection of the formulation of the governing partial differential

equations and the proper choice of discretization to produce sparse matrices with repetitive block structure. This structure is essential for efficiency of the inversion technique with a high degree of vectorizability in the solution phase. The goal was to develop a direct-solution technique for the 3-D unsteady Navier-Stokes equations for general geometries. This was based on the fact that direct-solution methodology developed by the principal investigators for 2-D unsteady Navier-Stokes equations has proved very robust and efficient.

After much careful study, the velocity-vorticity $(\bar{V},\bar{\omega})$ formulation has been selected, as opposed to the primitive-variable $(\bar{V},p)$ and the several vector-potential-vorticity $(\bar{A},\bar{\omega})$ formulations. All vector-potential formulations, which include stream-like functions, toroidal and poloidal potentials, etc., suffer from the necessity for more boundary conditions on the vector potential $\bar{A}$ than are available naturally from the physics of the flow problem. This difficulty can be traced to the fact that the vector potential is gauge invariant and 'extra' boundary conditions are required to uniquely select a specific gauge. Conversely, the non-physical boundary conditions selected must be consistent with a specific gauge function; otherwise, numerical convergence difficulties can be expected.

At first glance, the primitive-variable $(\bar{V},p)$ formulation appears to be computationally more efficient, since it requires the solution of only four unknowns, V_1, V_2, V_3, and p, rather than the six unknowns, V_1, V_2, V_3, ω_1, ω_2, and ω_3, occurring in the velocity-vorticity $(\bar{V},\bar{\omega})$ formulation. Indeed, much effort has been directed by the technical community at primitive-variable techniques for compressible flows. However, in the present effort,

it is determined that the velocity-vorticity $(\bar{V},\bar{\omega})$ problem can be discretized in such a manner as to produce a sparse matrix problem with repetitive block structure. As a result, the computational work associated with the implicit determination of one unknown can be effectively eliminated from the solution of the velocity problem, while the computational effort for yet another unknown can be eliminated from the vorticity-transport equation. Consequently, velocity-vorticity techniques deserve attention.

A philosophical point to bear in mind is that the $(\bar{V},\bar{\omega})$ formulation leads to a more natural decoupling of the governing equations than occurs in the primitive-variable technique. Specifically, pressure is an essential, nonlinear function of velocity, whereas vorticity is a linear function of velocity. Indeed, the $(\bar{V},\bar{\omega})$ formulation can physically separate the spin dynamics of a fluid particle (vorticity-transport problem) from the translational kinematics of the fluid particle (the elliptic velocity problem). This natural decoupling, which occurs in the $(\bar{V},\bar{\omega})$ formulation, may be seen to directly translate into simple and direct application of the necessary boundary conditions. Furthermore, complete internal consistency can be maintained with the $(\bar{V},\bar{\omega})$ formulation, i.e., all integral vorticity constraints, all integral velocity constraints, solenoidal velocity, etc., can be algebraically guaranteed, irrespective of grid size and time-step discretization, throughout the entire flow solution.

Wu [1985] and his associates, Fasel [1976], and Gatsky, Grosch and Rose [1982] have used the corresponding 2-D $(\bar{V},\bar{\omega})$ formulation and are presently developing 3-D algorithms using the $(\bar{V},\bar{\omega})$ formulation. The present analysis, however, aims to employ efficient direct inversion for the

elliptic velocity problem which can be formulated so as to produce a uniquely determined nonsingular vector-matrix problem with repetitive sparse block structure.

2.5 Pressure-Field Evaluation for Unsteady Flows

For unsteady flows analyzed using the (ω, ψ) formulation of the Navier-Stokes equations, the surface distribution of the pressure may be obtained by simply integrating the tangential component of the momentum equation along the surface. For determination of pressure in the total flow field, U. Ghia et al. [1976] have shown that a path-independent pressure field results only from the solution of the Neumann-Poisson pressure problem formed by the divergence of the momentum equations. With Neumann-type boundary conditions, this problem admits a solution, which is unique upto an arbitrary additive constant, only when the boundary values and the source in the differential equation satisfy Green's integral theorem. This places certain very specific requirements on the discretization of the Neumann-Poisson problem. This work is being pursued with the assistance of Collopy [1986] and comprises his Master's degree thesis, expected to be completed shortly. The application considered was the flow through an orifice in a doubly infinite circular pipe. The infinite extent of the flow domain in the streamwise direction necessitated additional considerations in order to maintain boundedness for the working variable for the pressure.

2.6 Supercomputer Usage and Graphical Post-Processing of Data

All of the research pursued towards this grant makes extremely extensive use of computer resources. For acceptable productivity, all available computer facilities are made use of, judiciously. During the

initial development stages, the programs are tested and run using the facilities of the University of Cincinnati (UC); these include the Aerospace Engineering Department's Perkin Elmer 3250 supermini computer system with dual processors for parallel computation possibility and the UC Computer Center's AMDAHL 470 V/7A mainframe facility. Most of the actual results are eventually generated using the NASA-Lewis CRAY XMP supercomputer system for the IPNS computations and the NASA-Langley CYBER 205 supercomputer system for the unsteady Navier-Stokes computations (2-D as well as 3-D). All four of these systems are equipped with their respective peripheral devices which are employed for post-processing the results of the computations and for presenting these results in suitable graphical form. All of the graphics packages employed are written by the present research team and are very efficient. However, the retrieval of the large data bases from the remotely located supercomputers is extremely inefficient via the present long-distance communication network. Therefore, plans are presently underway to purchase, through AFOSR funds, a superworkstation and, through the University of Cincinnati, have a leased direct-communication line to the NASA-Langley supercomputer site; this is most essential for the 3-D unsteady flow simulations, which are presently being pursued. The limited availability of supercomputer time continues to create a great deal of difficulties. Much valuable time is often expended in transferring programs from one computing facility to another, in the hope of expediency, but this necessitates continual changes in the programs and ends up consuming additional personnel time. Easier availability of larger amounts of supercomputer time would be most conducive for rapid progress in this research.

REFERENCES

Bouard, R. and Coutanceau, M., (1980), "The Early Stage of Development of the Wake Behind an Impulsively Started Cylinder for $40 < Re < 10^4$," Journal of Fluid Mechanics, Vol. 101, pp. 583-607.

Collopy, G.B., (1986), "Determination of Flow, Including Discharge Coefficients, in a Pipe-Orifice Using Unsteady Navier-Stokes Equations," M.S. Thesis, Department of Aerospace Engineering and Engineering Mechanics, University of Cincinnati, in progress.

Gatski, T.B., Grosch, C.E. and Rose, M.E., (1982), "A Numerical Study of the Two-Dimensional Navier-Stokes Equations in Vorticity-Velocity Variables," Journal of Computational Physics, Vol. 48, No. 1, pp. 1-22.

Fasel, H., (1976), "Investigation of the Stability of Boundary Layers by a Finite-Difference Model of the Navier-Stokes Equations," Journal of Fluid Mechanics, Vol. 78, Part 2, pp. 355-383.

Fornberg, B., (1985), "Steady Viscous Flow Past a Circular Cylinder Up to Reynolds Number 600," Journal of Computational Physics, Vol. 61, pp. 297-320.

Ghia, K.N. and Ghia, U., (1982), "Semi-Elliptic Globally-Iterative Analysis for Two-Dimensional Subsonic Internal Flows," presented at NASA-Lewis Workshop on Computational Fluid Mechanics, Cleveland, Ohio, October 1982.

Ghia, K.N., Osswald, G.A. and Ghia, U. (1985a), "Analysis of Two-Dimensional Incompressible Flow Past Airfoils Using Unsteady Navier-Stokes Equations," Proceedings of Third Symposium on Numerical and Physical Aspects of Aerodynamic Flows, Long Beach, California.

Ghia, K.N., Osswald, G.A. and Ghia, U., (1985b), "Simulation of Self-Induced Unsteady Motion in the Near-Wake of a Joukowski Airfoil," presented at First Nobeyama Workshop on High-Re Computations, Nobeyama, Japan, September 1985.

Ghia, K.N., Ghia, U., Osswald, G.A. and Liu, C.A., (1986), "Simulation of Separated Flow Past a Bluff Body Using Unsteady Navier-Stokes Equations," presented at I.U.T.A.M. Symposium on Boundary Layer Separation, London, England, August 1986.

Ghia, K.N., Osswald, G.A. and Ghia, U., (1986), "Simulation of Self-Induced Unsteady Motion in the Near-Wake of a Joukowski Airfoil," Lecture Notes in Engineering, November 1986.

Ghia, U., Ghia, K.N. and Ramamurti, R., (1983), "Hybrid C-H Grids for Turbomachinery Cascades," Advances in Grid Generation, ASME Publication, June 1983.

Ghia, U., Ghia, K.N., Rubin, S.G. and Khosla, P.K., (1981), "Study of Separated Flow in a Channel Using Primitive Variables," International Journal of Computers and Fluids, Vol. 9, pp. 123-142.

Ghia, U. and Goyal, R.K., (1976), "A Study of Laminar Incompressible Recirculating Flfow in a Driven Cavity of Polar Cross Section," Numerical/Laboratory/Cmputer Methods in Fluid Mechanics, ASME Publication, 1976.

Ghia, U., Ramamurti, R. and Ghia, K.N., (1985), "A Semi-Elliptic Analysis of Internal Viscous Flows," presented at First Nobeyama Workshop on High-Re Computations, Nobeyama, Japan, September 1985.

Ghia, U., Ramamurti, R. and Ghia, K.N., (1986), "A Semi-Elliptic Analysis of Internal Viscous Flows," Lecture Notes in Engineering, November 1986.

Grebogi, C., Ott, E. and Yorke, J.A., (1983), "Are Three-Frequency Quasiperiodic Orbits to be Expected in Typical Nonlinear Dynamical Systems?" Physical Review Letters, Vol. 51, No. 5, pp. 339-342.

Osswald, G.A., Ghia, K.N. and Ghia, U., (1985), "An Implicit Time-Marching Method for Studying Unsteady Flow with Massive Separation," AIAA CP 854, pp. 25-37.

Osswald, G.A., Ghia, K.N. and Ghia, U., (1986), "Simulation of Buffeting Stall for a Cambered Joukowski Airfoil Using a Fully Implicit Method," presented at 10th ICNMFD, Beijing, China; to appear in Lecture Notes in Physics, Editor: F.G. Zhuang, Springer Verlag, New York.

Smith, F.T., (1985), "A Structure for Laminar Flow Past a a Bluff Body at High Reynolds Number," Journal of Fluid Mechanics, Vol. 155, pp. 175-191.

Wu, J.C., (1985), "Computational and Theoretical Studies of Unsteady Viscous Aerodynamics," Proceedings of Conference on Low Reynolds Number Airfoil Aerodynamics, Notre Dame, Indiana.

SECTION 3

PAPERS AND REPORTS PUBLISHED

BOOKS AND MONOGRAPHS

Ghia, K.N. and Ghia, U., "Elliptic Systems: Finite-Difference Method," Chapter in Handbook on Numerical Heat Transfer, Editors: W.J. Minkowycz et al., John Wiley and Sons, 1987.

Ghia, U. and Ghia, K.N., "Navier-Stokes Equations for Incompressible Flow," Section of Chapter in Handbook of Fluids and Fluid Machinery, to be published in 1987.

Ghia, K.N., Osswald, G.A. and Ghia, U., "Analysis of Two-Dimensional Incompressible Flow Past Airfoils Using Unsteady Navier-Stokes Equations," Chapter in Numerical and Physical Aspects of Aerodynamic Flows: Vol. III, Editor: T. Cebeci, Springer-Verlag, New York, December 1986.

PAPERS AND REPORTS

Ghia, K.N., Ghia, U. and Shin, C.T., "Study of Asymptotic Incompressible Flow in Curved Ducts Using a Multi-Grid Technique," to appear in Journal of Fluids Engineering, June 1987.

Ghia, K.N., Ghia, U., Osswald, G.A. and Liu, C.A., "Simulation of Separated Flow Past a Bluff Body Using Unsteady Navier-Stokes Equations," to appear in Boundary Layer Separation, Editors: F.T. Smith and S. Brown, North Holland, 1987.

Ghia, K.N., Ghia, U., Liu, C.A. and Osswald, G.A., "Study of Unsteady Wake Behind Circular Cylinder Using Time-Dependent Simulation," Bulletin of the American Physical Society, Vol. 31, No. 10, November 1986.

Osswald, G.A., Ghia, K.N. and Ghia, U., "Simulation of Buffeting Stall for a Cambered Joukowski Airfoil Using a Fully Implicit Method," Lecture Notes in Physics, Editors: F.G. Zhuang and Y.L. Zhu, Vol. 264, pp. 516-522, Springer Verlag, 1986.

Ghia, K.N., Osswald, G.A. and Ghia, U., "Simulation of Self-Induced Motion in the Near-Wake of a Joukowski Airfoil," Lecture Notes in Engineering; Editor: K. Kuwahara, Springer-Verlag, New York, November 1986.

Ghia, U., Ramamurti, R. and Ghia, K.N., "A Semi-Elliptic Analysis of Internal Viscous Flows," Lecture Notes in Engineering; Editor: K. Kuwahara, Springer-Verlag, New York, September 1986.

Osswald, G.A., Ghia, K.N. and Ghia, U., "An Implicit Time-Marching Method for Studying Unsteady Flow with Massive Separation," AIAA CP 854, July 1985.

McGreehan, W.F., Ghia, K.N., Ghia, U. and Osswald, G.A., "Analysis of Separated Flow in a Pipe Orifice Using Unsteady Navier-Stokes Equations," Lecture Notes in Physics, Edited by Soubaramayer and J. Boujot, Vol. 218, p. 393-, 1985.

SECTION 4

SCIENTIFIC INTERACTIONS - SEMINARS AND PAPER PRESENTATIONS

SEMINARS AND INVITED LECTURES

Ghia, K.N., Ghia, U., Osswald, G.A. and Liu, C.A., "Simulation of Separated Flow Past a Bluff Body Using Unsteady Navier-Stokes Equations," presented at I.U.T.A.M. Symposium on Boundary Layer Separation, London, England, August 1986.

Ghia, K.N., "Simulation of Self-Excited, Vortex Dominated Massively Separated Viscous Flow Using Unsteady Navier-Stokes Equations," presented at University of Southern California, Los Angeles, California, July 1986.

Ghia, K.N., "Study of Unsteady Self-Excited Massively Separated Flows," presented at Georgia Institute of Technology, Atlanta, Georgia, May 1986.

Ghia, K.N., "Study of High-Incidence Vortex Dominated Flows," presented at Rockwell International Science Center, Thousand Oaks, California, January 1986.

Ghia, K.N., "Two-Dimensional and Axisymmetric Self-Excited Oscillatory Separated Viscous Flows," presented at Indian Institute of Technology, Bombay, India, September 1985.

Ghia, K.N. and Ghia, U., "Navier-Stokes Solutions of Some Low-Speed Viscous Flows," presented at Institute for Computational Fluid Dynamics, Tokyo, Japan, September 1985.

Ghia, K.N., "Simulation of Self-Induced Motion in the Near-Wake of a Joukowski Airfoil," presented at First Nobeyama Workshop on High Reynolds Number Flow Computations, Nobeyama, Japan, September 1985.

Ghia, K.N., "On an Adaptive Grid Technique and Simulation of High Reynolds Number Flows Using Fully Implicit Technique," presented at ICASE, NASA Langley Research Center, Hampton, VA, August 1985.

Ghia, K.N., "On High Curvature Resolution Problems in Adaptive Grid and Bifurcation Solutions in Viscous Flows," presented at Supersonic Computational Fluid Dynamics Branch, NASA Langley Research Center, Hampton, VA, August 1985.

Ghia, U., "Inclusion of Upstream Influence in Parabolized Navier-Stokes Equations for Low-Speed Viscous Flows with Complex Geometry," presented at University of Southern California, Los Angeles, California, July 1986.

Ghia, U., "Study of Viscous Flow Problems with Complex Geometry, Using an Interacting Parabolized Navier-Stokes Analysis," presented at Georgia Institute of Technology, Atlanta, Georgia, May 1986.

Ghia, U., "Analysis of Flows in Turbomachinery Applications Using an Interacting Parabolized Navier-Stokes Formulation," presented at Indian Institute of Technology, Bombay, India, September 1985.

Ghia, U., "Interacting Parabolized Navier-Stokes Formulation," presented at ICASE, NASA-Langley Research Center, Hampton, VA, August 1985.

Ghia, U., "Analysis of Turbulent Boundary Layer Flow Over Roughened Surfaces," presented at Supersonic Computational Fluid Dynamics Branch, NASA-Langley Research Center, Hampton, Virginia, August 1985.

PAPER PRESENTATIONS

Liu, C., Ghia, K.N., Ghia, U. and Osswald, G.A., "On Unsteady Viscous Flow Past a Circular Cylinder," presented at AIAA 12th Annual Mini-Symposium on Aerospace Science and Technology, WPAFB, Ohio, March 1986.

Osswald, G.A., Ghia, K.N. and Ghia, U., "Unsteady Navier-Stokes Analysis of Viscous Flow Past a Cambered Joukowski Airfoil," presented at AIAA 12th Annual Mini-Symposium on Aerospace Science and Technology, WPAFB, Ohio, March 1986.

Osswald, G.A, Ghia, K.N. and Ghia, U., "Simulation of Buffeting Stall for a Cambered Joukowski Airfoil Using a Fully Implicit Method," presented at Tenth International Conference on Numerical Methods in Fluid Dynamics, Beijing, China, June 1986.

Ramamurti, R., Ghia, U. and Ghia, K.N., "Hybrid C-H Grids and a Semi-Elliptic Solution of Viscous Flow for Cascades," in AIAA Paper 85-1535, July 1985.

SECTION 5

STUDENT THESES AND DISSERTATIONS

M.S. DEGREE THESES

Collopy, G.B., "Determination of Flow Including Discharge Coefficients, In a Pipe-Orifice Using Unsteady Navier-Stokes Equations," M.S. Thesis, Department of Aerospace Engineering and Engineering Mechanics, University of Cincinnati, Cincinnati, Ohio, August 1987.

Liu, C.A., "Study of a Two-Dimensional Viscous Flow Past a Circular Cylinder Using Unsteady Navier-Stokes Equations," M.S. Thesis, Department of Aerospace Engineering and Engineering Mechanics, University of Cincinnati, Cincinnati, Ohio, August 1987.

Ph.D. DEGREE DISSERTATIONS

Ramamurti, R., "A Semi-Elliptic Analysis and Hybrid C-H Grids for Two-Dimensional Viscous Flow Through Cascades," Ph.D. Dissertation, Department of Aerospace Engineering and Engineering Mechanics, University of Cincinnati, Cincinnati, Ohio, August 1986.

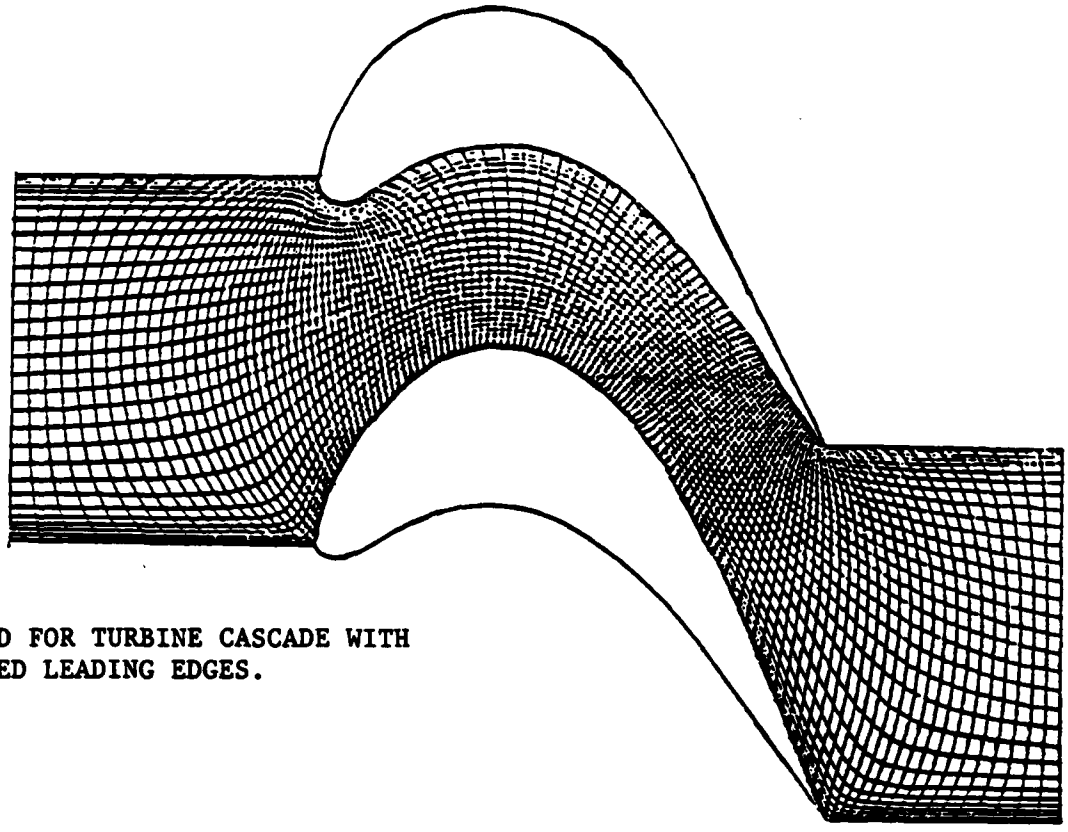

FIG. 1. H-GRID FOR TURBINE CASCADE WITH ROUNDED LEADING EDGES.

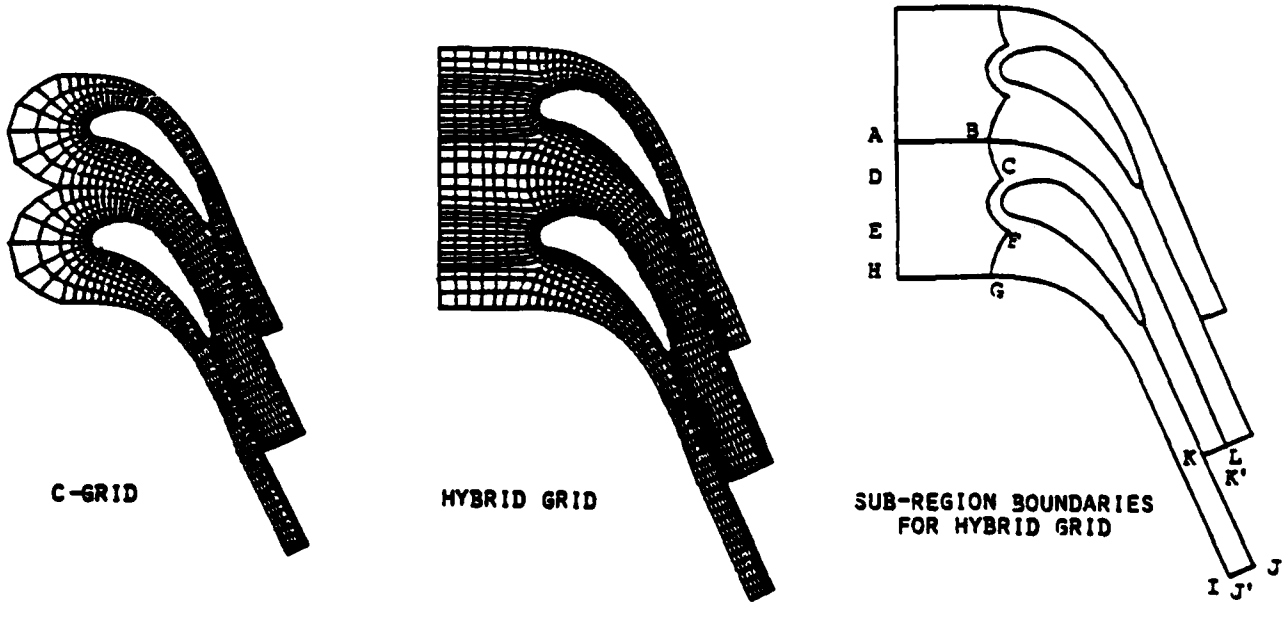

FIG. 2. HYBRID C-H GRID FOR CASCADE - PATCHED SOLUTION.

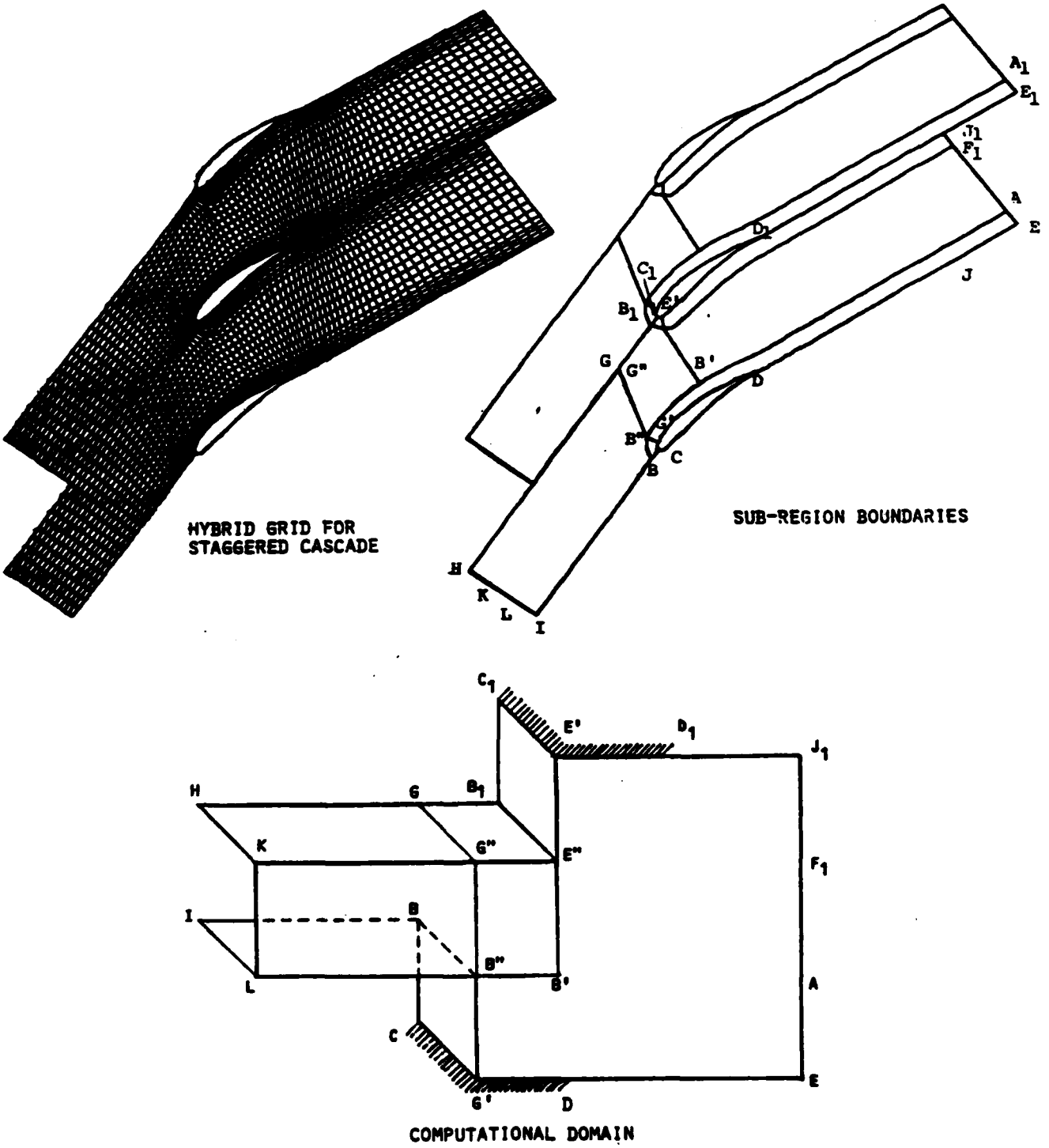

FIG. 3. COMPUTATIONAL DOMAIN (3-D) FOR HYBRID GRID FOR HIGHLY STAGGERED CASCADE.

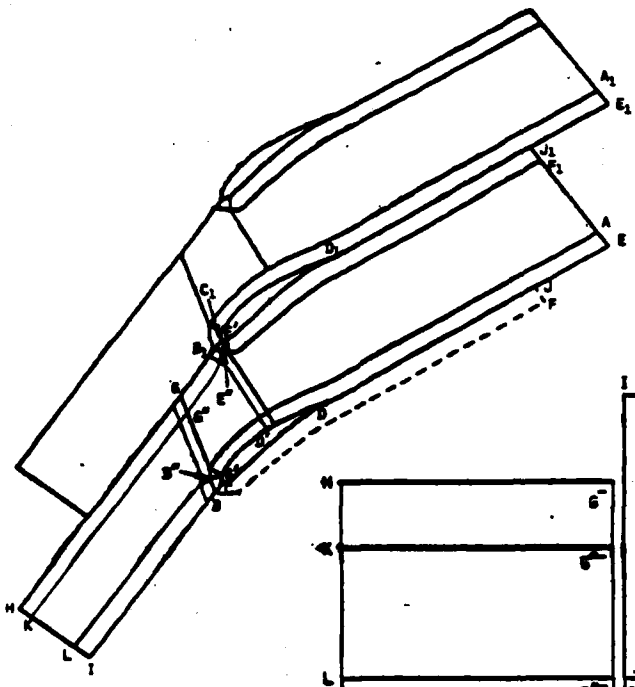

FIG. 4. SUB-REGION BOUNDARIES FOR HYBRID GRID.

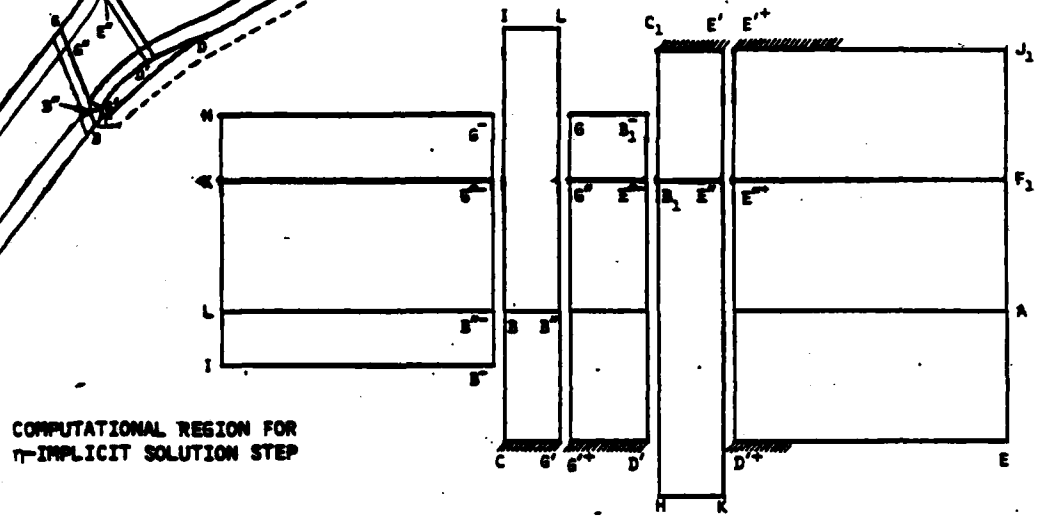

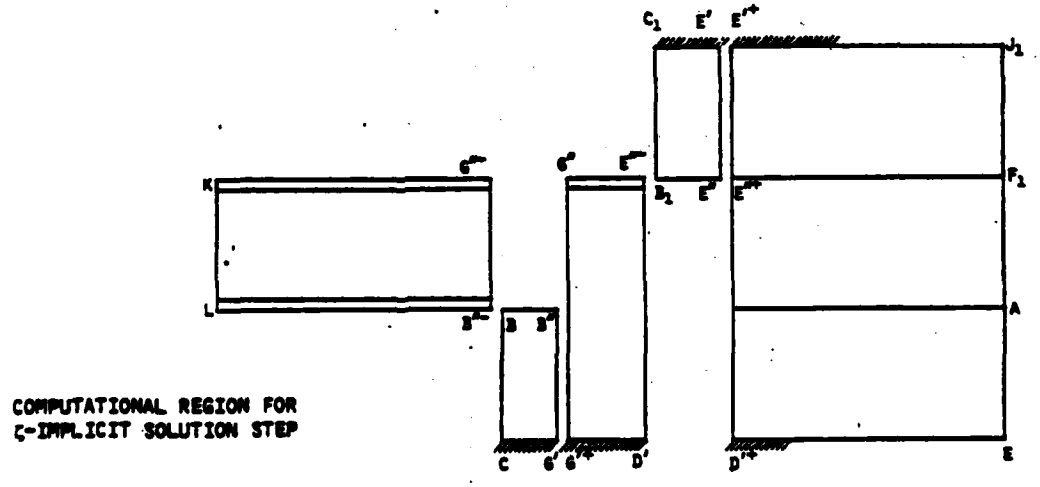

FIG. 5. 2-D COMPUTATIONAL REGIONS FOR APPLICATION OF ADI SCHEME TO HYBRID GRID FOR COMPOSITE SOLUTION.

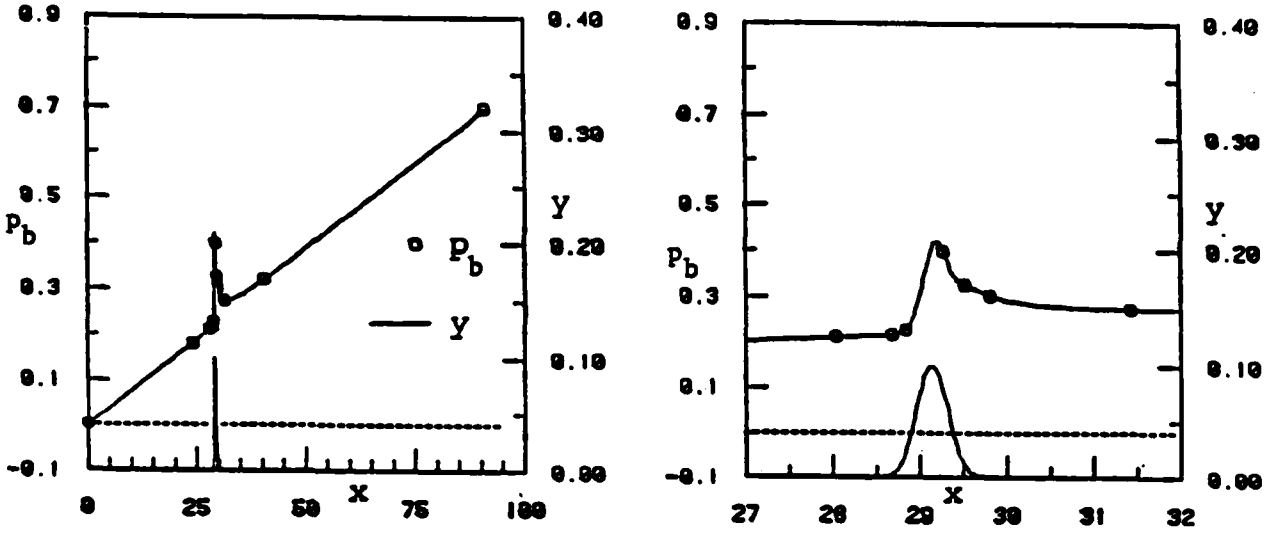

ENLARGED HORIZONTAL SCALE

SURFACE PRESSURE DISTRIBUTION

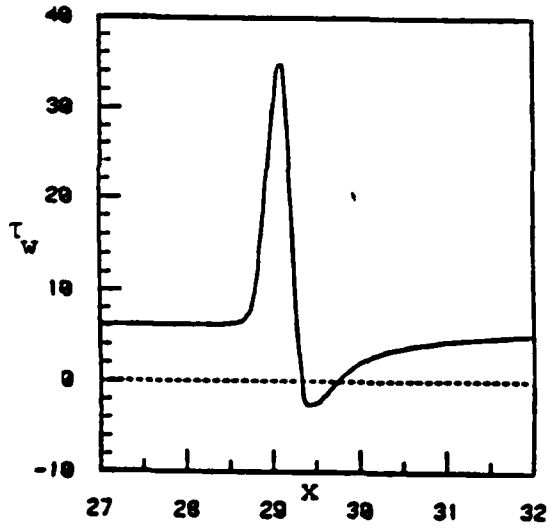

SURFACE SHEAR PARAMETER

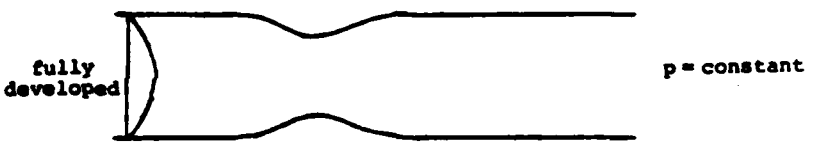

GEOMETRY AND
INFLOW AND OUTFLOW BOUNDARY CONDITIONS

FIG. 6 . RESULTS FOR SYMMETRIC CHANNEL WITH EXPONENTIAL CONSTRICTION; Re = 1500, t_{max}/h = 0.2, (201 x 61) GRID.

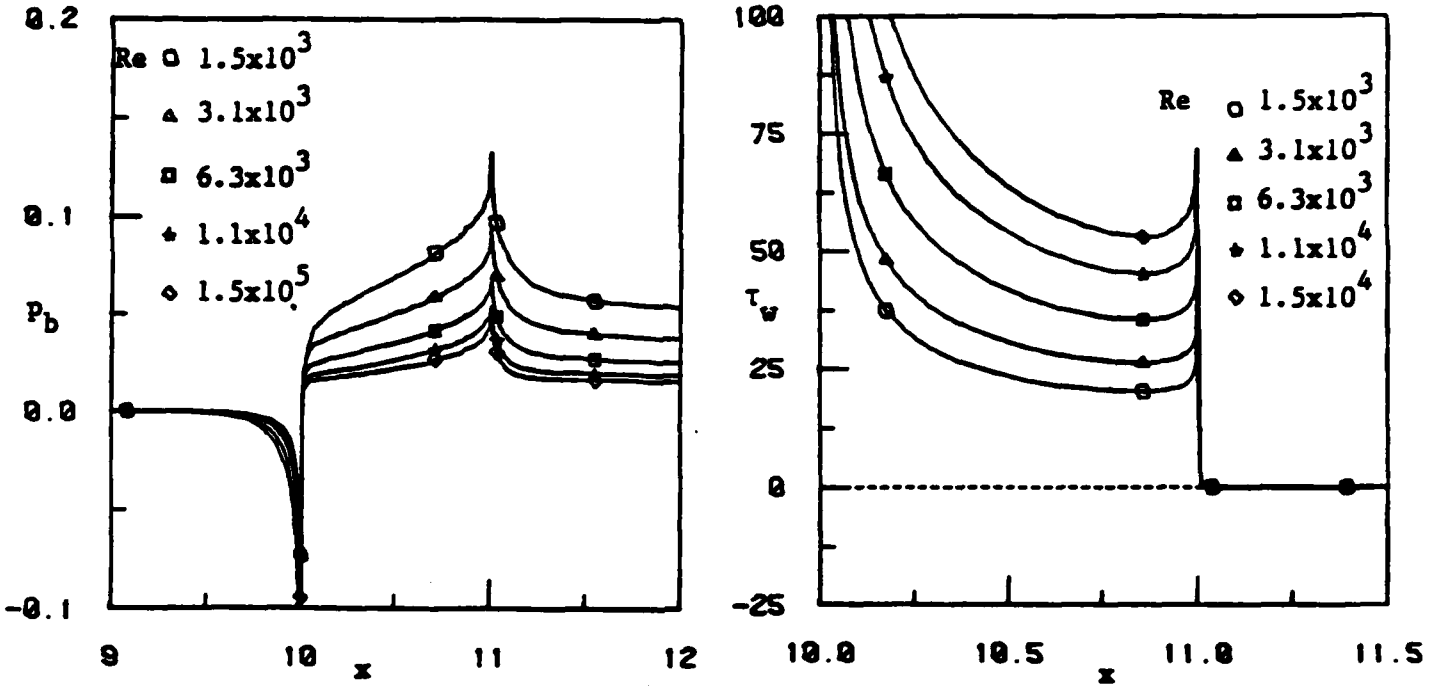

FIG. 7. RESULTS FOR FLAT-PLATE CASCADE FOR VARIOUS REYNOLDS NUMBERS, (186 x 71) GRID.

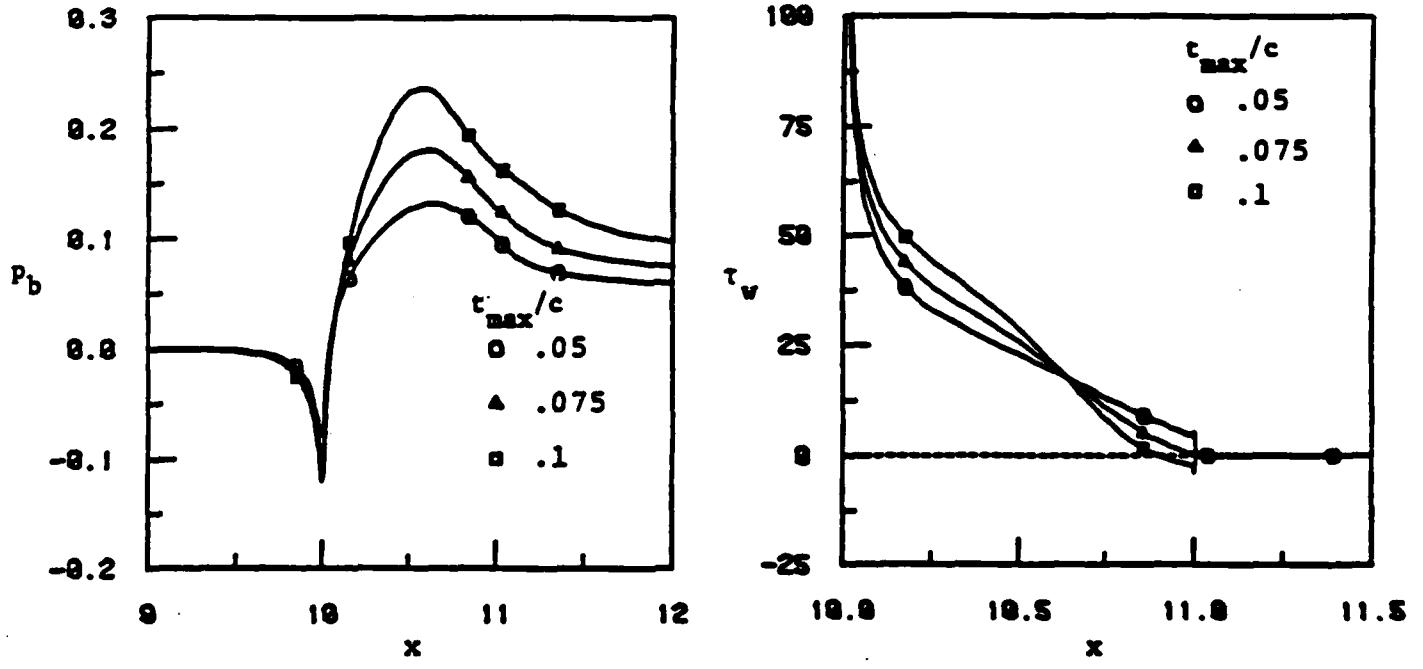

FIG. 8a. RESULTS FOR SYMMETRIC CASCADE OF PARABOLIC AIRFOILS FOR VARIOUS t_{max} /c; Re = 1500, (186 x 71) GRID.

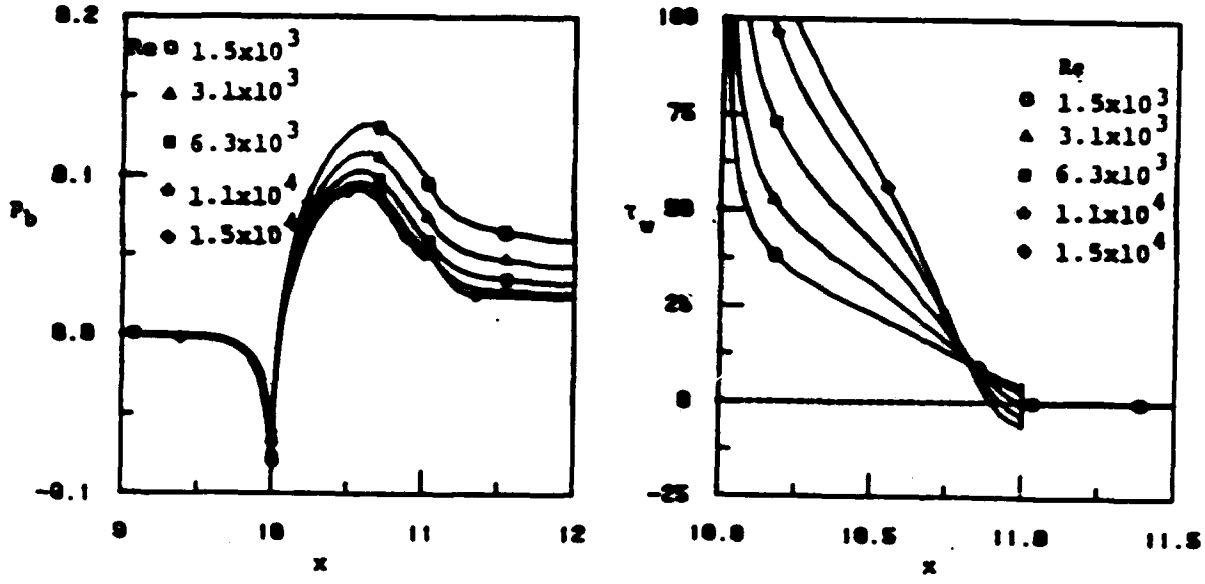

FIG. 8b. RESULTS FOR SYMMETRIC CASCADE OF PARABOLIC AIRFOILS FOR VARIOUS REYNOLDS NUMBERS; $t_{max}/c = 0.05$, (186 x 71) GRID.

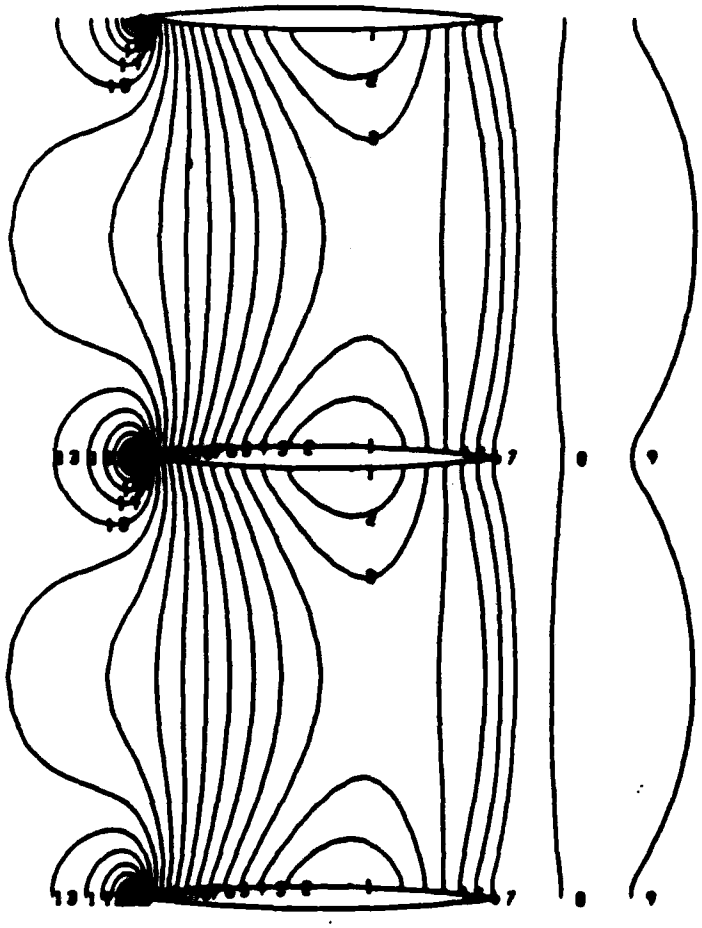

NO.	VALUE
1	0.292266 01
2	0.293136 01
3	0.294006 01
4	0.294876 01
5	0.295746 01
6	0.296626 01
7	0.297496 01
8	0.298366 01
9	0.299236 01
10	0.300116 01
11	0.300986 01
12	0.301856 01
13	0.302726 01
14	0.303596 01
15	0.304476 01
16	0.305346 01
17	0.306216 01
18	0.307086 01
19	0.307966 01
20	0.308836 01
21	0.309706 01

FIG. 8c. PRESSURE CONTOURS FOR SYMMETRIC CASCADE OF PARABOLIC AIRFOILS; $t_{max}/c = 0.05$, $M_\infty = 0.49$, Re = 15,000.

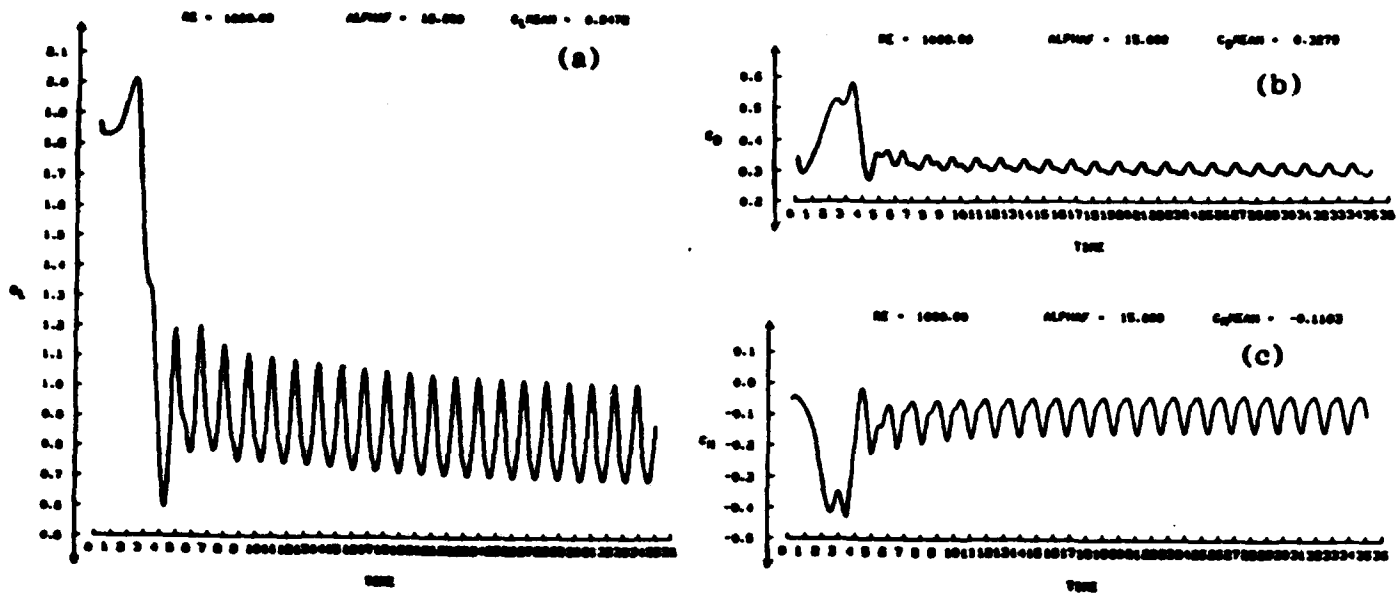

Fig. 9. Instantaneous Aerodynamic Coefficients at Re = 1,000, $\alpha_f = 15°$. (a) Lift C_L. (b) Drag C_D. (c) Moment C_M. - Symmetric Joukowski Airfoil.

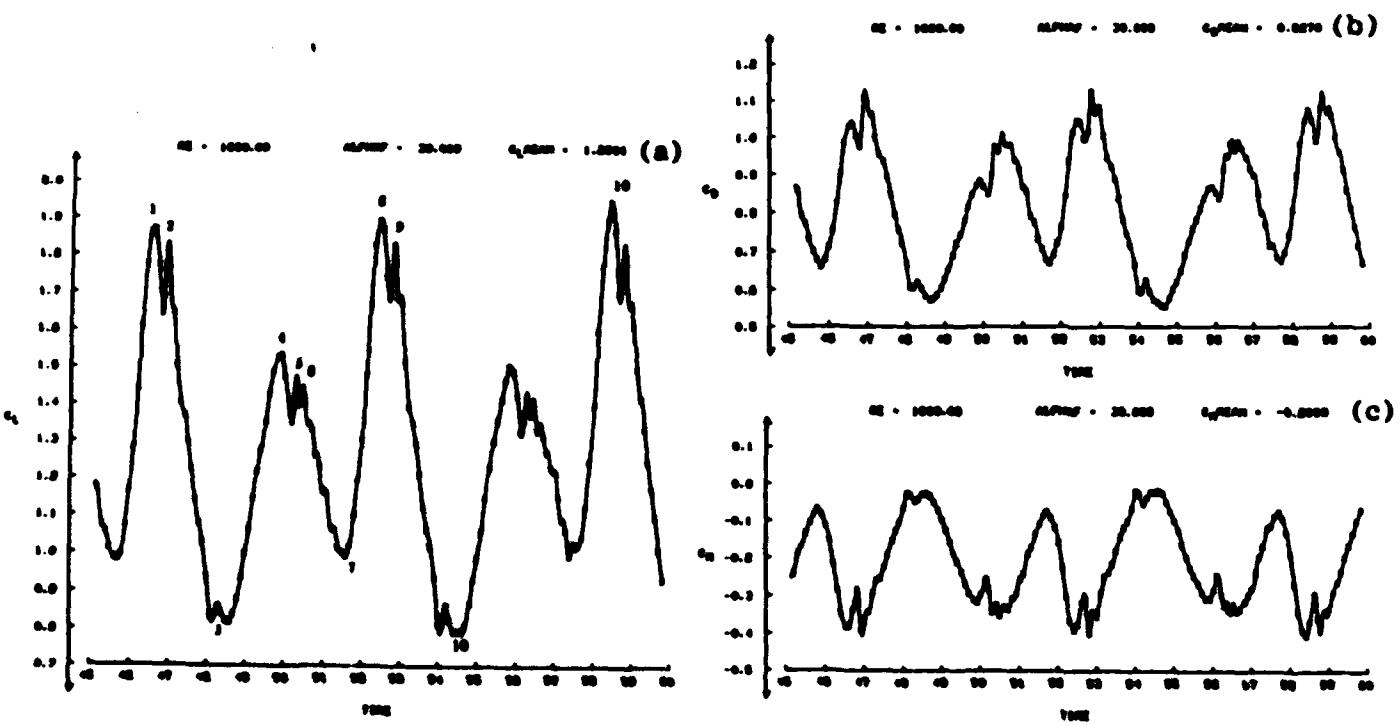

Fig. 10. Instantaneous Aerodynamic Coefficients at Re = 1,000, $\alpha_f = 30°$. (a) Lift C_L. (b) Drag C_D. (c) Moment C_M. - Symmetric Joukowski Airfoil.

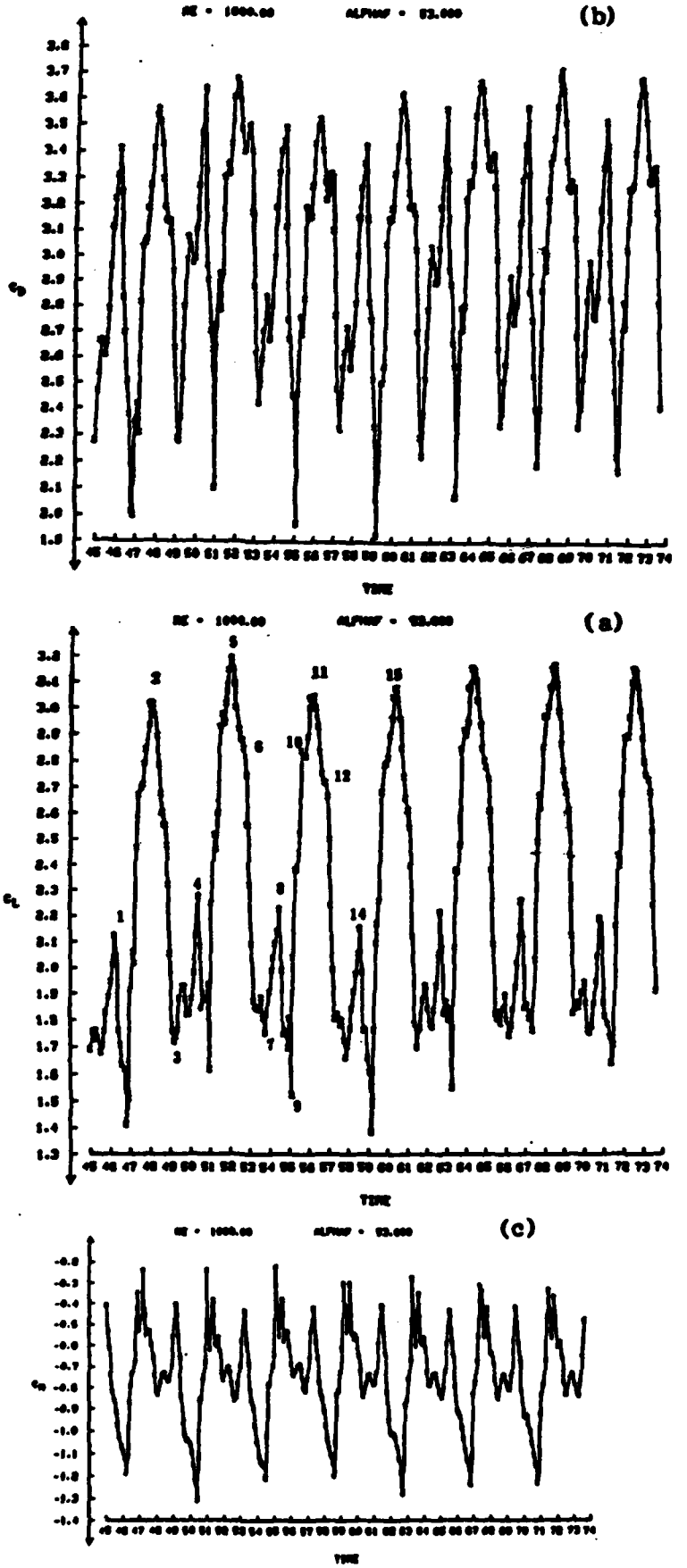

Fig. 11 Instantaneous Aerodynamic Coefficients at Re = 1,000, α_f = 53°. (a) Lift C_L, (b) Drag C_D, (c) Moment C_M. - Symmetric Joukowski Airfoil.

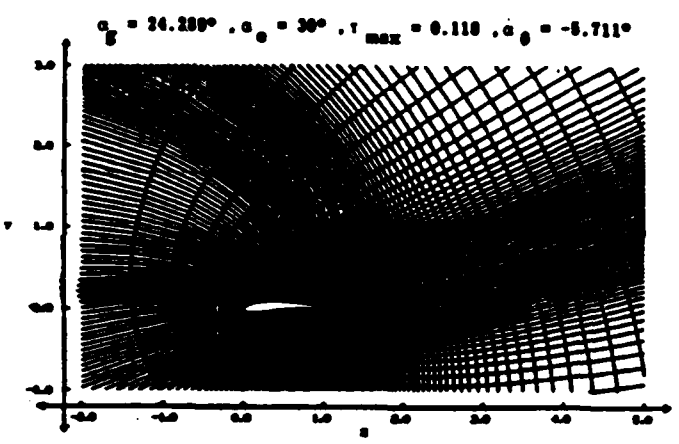

Fig. 12 Typical Grid Distribution for Göttingen 580 Airfoil.

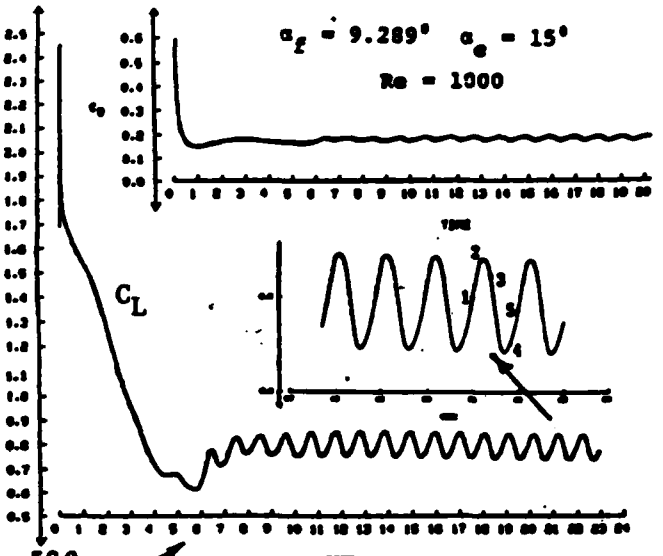

Fig. 14 Lift and Drag Histories; Göttingen 580.

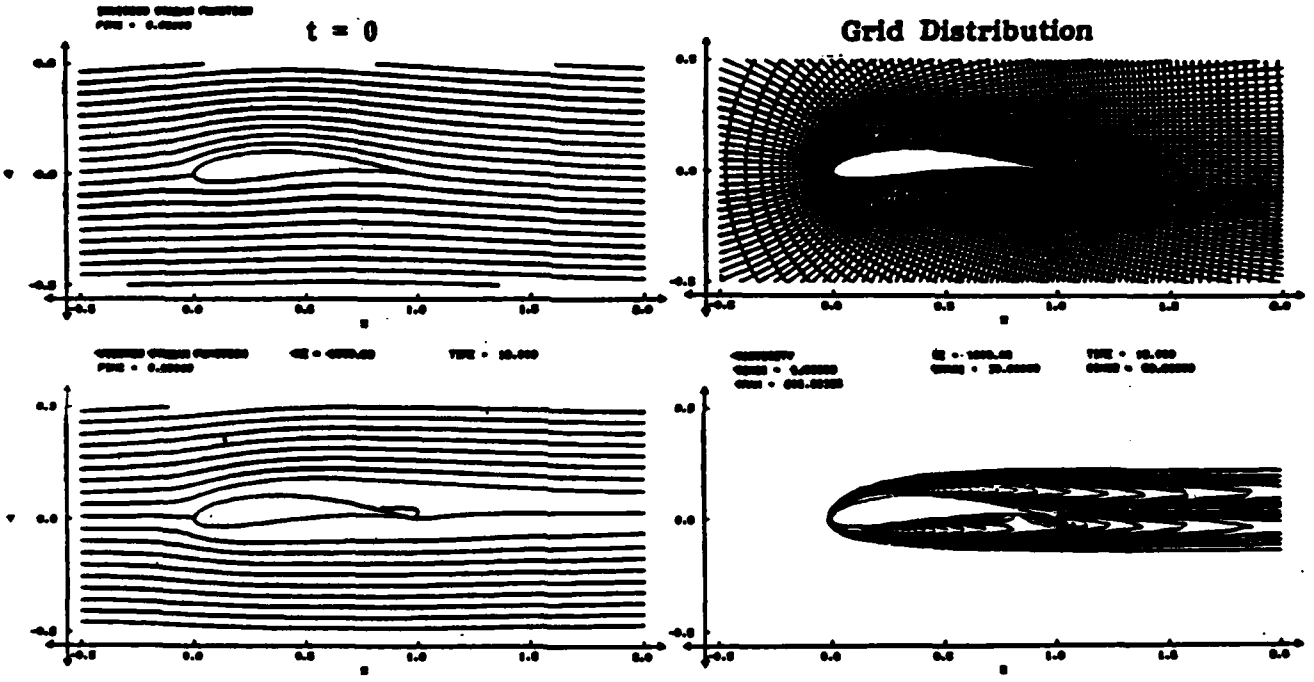

Fig. 13 Göttingen 580 at Re = 1000, α_e = 5.711°; at t = 0: Inviscid Stream Function and Grid Distribution, at t = 18.0 Steady-State Solution.

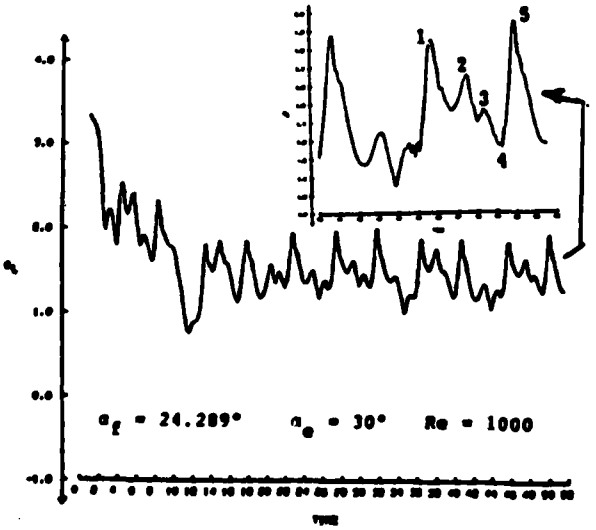

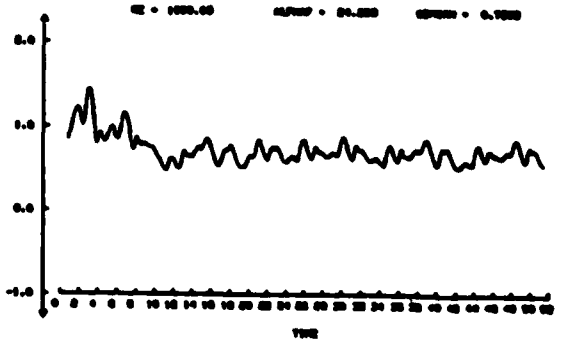

Fig. 15 Lift and Drag Histories; Göttingen 580.

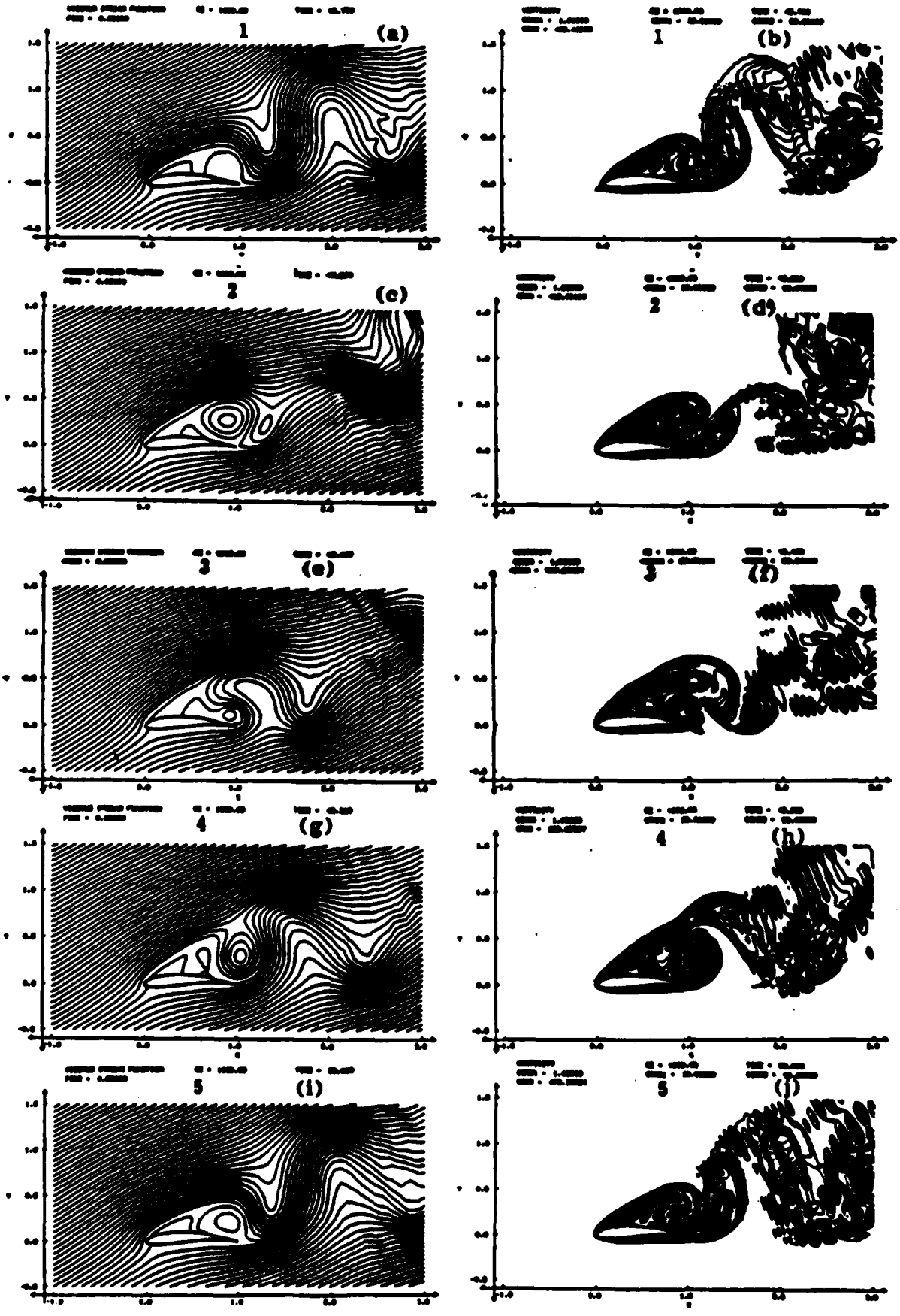

INSTANTANEOUS STREAM-FUNCTION CONTOURS VORTICITY CONTOURS

Fig. 16. TE-LE-TE Vortex-Shedding Cycle for Göttingen 580 Airfoil at Re = 1000, α_e = 30°.

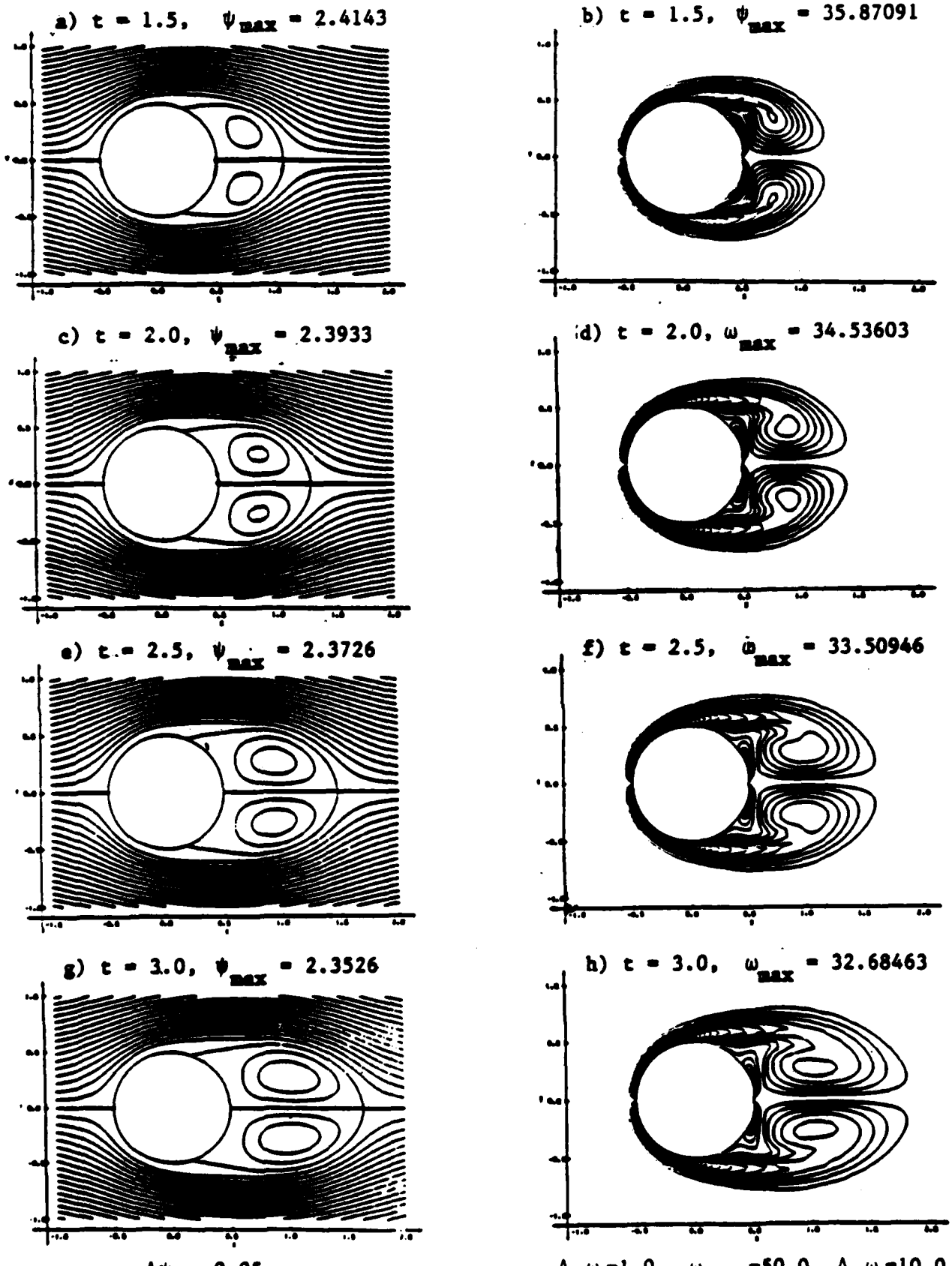

$\Delta\psi$ = 0.05

INSTANTANEOUS STREAM-FUNCTION CONTOURS

$\Delta_1\omega$ = 1.0, ω_{max1} = 50.0, $\Delta_2\omega$ = 10.0

VORTICITY CONTOURS

FIG. 17 DEVELOPMENT OF FLOW PAST CYLINDER AT Re = 200; SYMMETRY NOT ASSUMED.

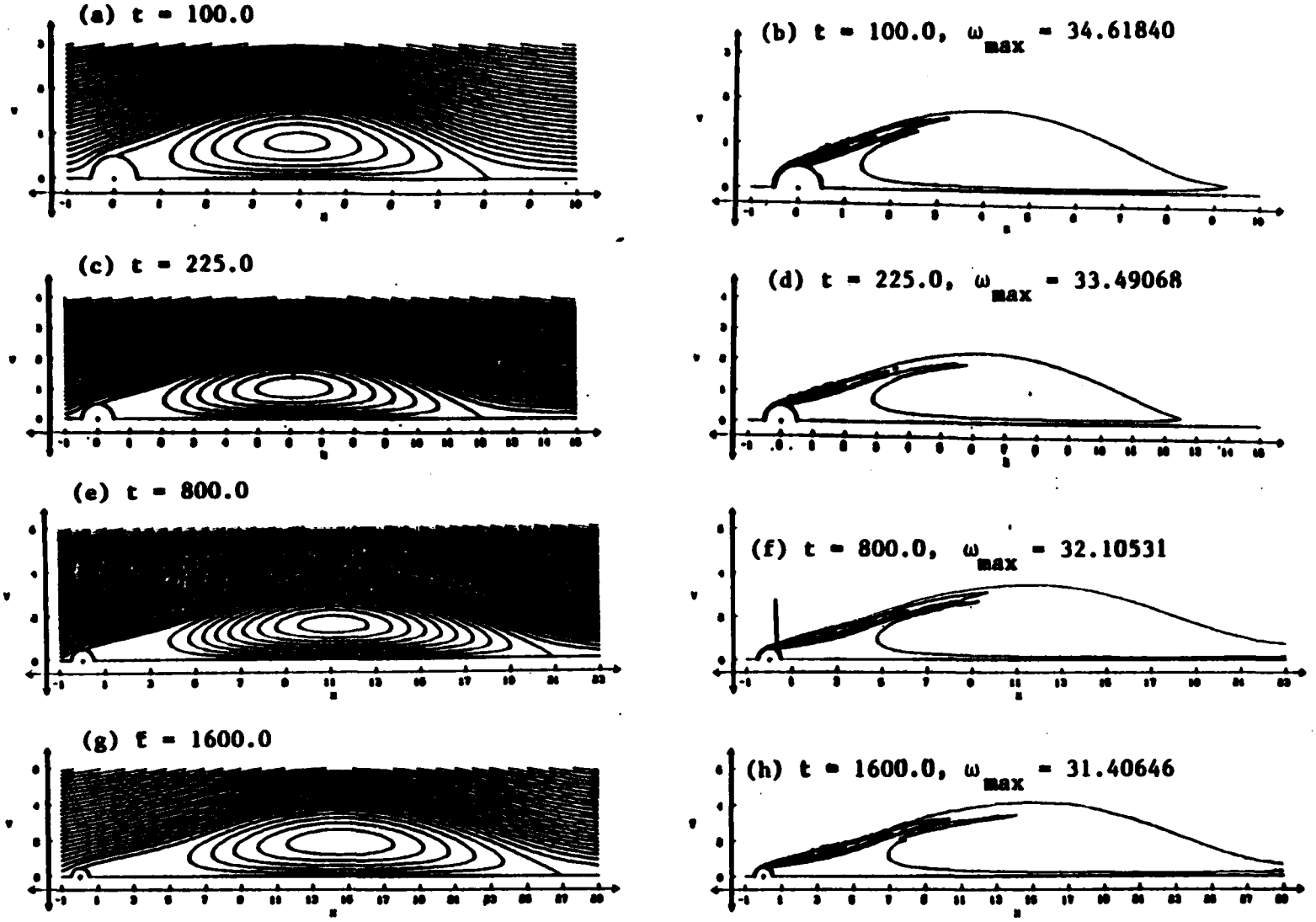

$\Delta\psi = 0.1$

INSTANTANEOUS STREAM-FUNCTION CONTOURS

$\Delta_1\omega$=1.0, ω_{max1}=50.0, $\Delta_2\omega$ =50.0

VORTICITY CONTOURS

FIG. 18 DEVELOPMENT OF SYMMETRIC FLOW PAST CYLINDER AT Re = 500.

END

DATE
FILMED

DEC.

1987